

Electronic Supplementary Information

Understanding the magnetism of {Fe₂Ln} dimers, step-by-step

Svetlana G. Baca, Jan van Leusen, Manfred Speldrich, and Paul Kögerler*

Experimental Section

Materials and General Methods. All reactions were carried out under aerobic conditions using commercial grade solvents. [Fe₃O(O₂CCMe₃)₆(EtOH)₃]NO₃·EtOH was prepared by a slightly modified procedure reported in ref. 1. Commercially available N-butyldiethanolamine was used without further purification. IR spectra (4000–400 cm⁻¹) were recorded on a Perkin-Elmer Spectrum One spectrometer using KBr pellets. TGA/DTA measurements were carried out with a Mettler Toledo TGA/SDTA 851 in dry N₂ (60 mL min⁻¹) at a heating rate of 5 K min⁻¹; TGA/DTA curves for **1–4** are shown in Figs. S15–S17. Magnetic susceptibility data were recorded using a Quantum Design MPMS-5XL SQUID magnetometer for direct current (DC) as well as alternating current (AC) measurements. Microcrystalline samples were pressure-compacted and immobilized into cylindrical PTFE sample holders. Experimental data were corrected for sample holder and diamagnetic contributions calculated from tabulated values.

Single-crystal X-ray diffraction experiments were carried out on a Bruker diffractometer with APEX II CCD detector using graphite monochromated MoK_α radiation at 100 K for all compounds. The summary of the data collection and the crystallographic parameters of compounds **1–4** are listed in Table S1. The positions of metal atoms were found by the direct methods. The remaining atoms were located in an alternating series of least-squares cycles and difference Fourier maps. All non-hydrogen atoms were refined in full-matrix anisotropic approximation using the SHELX suite of programs.² H-atoms of OH groups and the coordinated water molecules have been located from Fourier difference maps and fixed to their position. The remaining hydrogen atoms were placed in the structure factor calculation at idealized positions and were allowed to ride on the neighboring atoms with relative isotropic displacement coefficients. In **1**, the solvent ethanol molecules as well as some of the methyl and methylene groups in N-butyldiethanolamine ligands and the methyl groups in pivalates were found to be

disordered; therefore, various restraints (SIMU, DELU, SADI, DFIX) were applied to obtain reasonable geometrical parameters and thermal displacement coefficients. Badly disordered ethanol molecules in **2** were removed by the SQUEEZE routine. Compounds **3** and **4** form non-merohedrally twinned crystals, and their data sets were treated with the programs CELL_NOW³ and TWINABS.⁴ Both components of the twin were indexed with the program CELL_NOW. Using all reflection data, integrated intensities for the reflections from two components were written into HKLF 5 reflection files. Selected bond distances and angles for **1–4** are listed in Tables S2, S4, S6 and S8, hydrogen bonding interactions in **1–4** are detailed in Tables S3, S5, S7 and S9. The Diamond [Diamond Version 4.2.0, 1997-2016, Crystal Impact GbR, Bonn, Germany] software suite was used for graphical representations. The asymmetric units for **1** and **3** with atomic numbering scheme are shown in Figs. S1 and S5; the molecular structures of **1** and **3** with hydrogen bonding interactions are shown in Figs. S2 and S6, and packing diagrams for compound **1** in Figs. S3 and S4, for compound **3** in Figs. S7 and S8.

Synthesis of $[\text{Fe}_4\text{Dy}_2(\text{OH})_2(\text{N}_3)_2(\text{bdea})_4(\text{O}_2\text{CCMe}_3)_5(\text{H}_2\text{O})]\text{NO}_3 \cdot 2(\text{EtOH})$ (1). A solution containing $[\text{Fe}_3\text{O}(\text{O}_2\text{CCMe}_3)_6(\text{EtOH})_3]\text{NO}_3 \cdot \text{EtOH}$ (0.208 g, 0.2 mmol), $\text{Dy}(\text{NO}_3)_3 \cdot 6\text{H}_2\text{O}$ (0.3 mmol), NaN_3 (0.038 g, 0.6 mmol) and H_2bdea (0.084 g, 0.6 mmol) in 10 mL EtOH was heated under reflux for 30 min and then filtered. The filtrate was kept in the closed vial under room temperature. After two weeks the yellow crystals of **1** suitable for X-ray analysis were filtered off, washed with EtOH, water, MeCN and dried in air. Yield (based on Fe): 0.150 g, 53%. Crystals of **1** decompose without solvent. Elemental analysis calcd. for **1** without solvent molecules, $\text{C}_{57}\text{H}_{117}\text{Dy}_2\text{Fe}_4\text{N}_{11}\text{O}_{24}$ (1888.98 g mol⁻¹): C 36.24, H 6.27, N 8.16%; found: C 36.17, H 6.57, N 8.17%. IR (KBr pellet, cm⁻¹): $\nu = 3420$ (br, m), 2959 (m), 2930 (w), 2870 (m), 2061 (vs), 1597 (m), 1556 (vs), 1483 (s), 1458 (m), 1416 (s), 1374 (m), 1355(m), 1330(w), 1296 (w), 1226 (m), 1082 (m), 1039 (sh), 983 (w), 894 (w), 877(sh), 785 (w), 636 (sh), 607 (sh), 586 (m), 546 (w), 427 (m).

Synthesis of $[\text{Fe}_4\text{Y}_2(\text{OH})_2(\text{N}_3)_2(\text{bdea})_4(\text{O}_2\text{CCMe}_3)_5(\text{H}_2\text{O})]\text{NO}_3 \cdot 2(\text{EtOH})$ (2). This compound was prepared in a similar way to **1**, but using $\text{Y}(\text{NO}_3)_3 \cdot 6\text{H}_2\text{O}$ instead of $\text{Dy}(\text{NO}_3)_3 \cdot 6\text{H}_2\text{O}$. Yield (based on the $\{\text{Fe}_3\}$ precursor): 0.054 g, 21%. Crystals of **2** also quickly decompose without solvent. Elemental analysis calcd. for **2** without solvent molecules, $\text{C}_{57}\text{H}_{117}\text{Fe}_4\text{N}_{11}\text{O}_{24}\text{Y}_2$ (1741.79

g mol^{-1}): C 39.30, H 6.77, N 8.85%; found: C 38.96, H 6.75, N 8.81%. IR (KBr pellet, cm^{-1}): $\nu =$ 3374 (br, m), 2959 (m), 2929 (w), 2871 (m), 2062 (vs), 1599 (m), 1556 (vs), 1483 (s), 1458 (m), 1417 (s), 1374 (m), 1356(m), 1330(w), 1299 (w), 1226 (m), 1081 (m), 1038 (sh), 982 (w), 893 (w), 877(sh), 785 (w), 636 (sh), 607 (sh), 586 (m), 545 (w), 427 (m).

Synthesis of $[\text{Fe}_4\text{Gd}_2(\text{OH})_2(\text{N}_3)_2(\text{bdea})_4(\text{O}_2\text{CCMe}_3)_4(\text{NO}_3)_2] \cdot 3(\text{EtOH})$ (3). This complex was prepared analogous to **1**, but using $\text{Gd}(\text{NO}_3)_3 \cdot 6\text{H}_2\text{O}$ instead of $\text{Dy}(\text{NO}_3)_3 \cdot 6\text{H}_2\text{O}$. Yield (based on the $\{\text{Fe}_3\}$ precursor): 0.110 g, 40%. Crystals of **3** also quickly decompose without solvent. Elemental analysis calcd. for **3** without solvent molecules, $\text{C}_{52}\text{H}_{106}\text{Fe}_4\text{Gd}_2\text{N}_{12}\text{O}_{24}$ (1821.34 g mol^{-1}): C 34.29, H 5.87, N 9.23%; found: C 33.26, H 5.88, N 8.96%. IR (KBr pellet, cm^{-1}): $\nu =$ 3606 (m), 3382 (br, m), 2959 (m), 2930 (w), 2871 (m), 2063 (vs), 1597 (m), 1548 (vs), 1483 (s), 1458 (m), 1407 (s), 1374 (m), 1358(m), 1330(w), 1289 (w), 1225 (m), 1079 (m), 1034 (sh), 984 (w), 895 (w), 817(sh), 789 (w), 738 (w), 633 (sh), 604 (sh), 583 (m), 544 (w), 427 (m).

Synthesis of $[\text{Fe}_4\text{Eu}_2(\text{OH})_2(\text{N}_3)_2(\text{bdea})_4(\text{O}_2\text{CCMe}_3)_4(\text{NO}_3)_2] \cdot 3(\text{EtOH})$ (4). This complex was prepared analogous to **1**, but using $\text{Eu}(\text{NO}_3)_3 \cdot 6\text{H}_2\text{O}$ instead of $\text{Dy}(\text{NO}_3)_3 \cdot 6\text{H}_2\text{O}$. Yield (based on the $\{\text{Fe}_3\}$ precurs): 0.125 g, 46%. Crystals of **4** also quickly decompose without solvent. Elemental analysis calcd. for **4** without solvent molecules, $\text{C}_{52}\text{H}_{106}\text{Eu}_2\text{Fe}_4\text{N}_{12}\text{O}_{24}$ (1810.77 g mol^{-1}): C 34.49, H 5.90, N 9.28%; found: C 33.59, H 5.91, N 9.06 %. IR (KBr pellet, cm^{-1}): $\nu =$ 3604 (m), 3376 (br, m), 2959 (m), 2929 (w), 2870 (m), 2062 (vs), 1591 (m), 1547 (vs), 1482 (s), 1407 (s), 1374 (m), 1359(m), 1332(m), 1291 (m), 1226 (m), 1078 (m), 1034 (sh), 974 (w), 894 (w), 817(sh), 789 (w), 736 (w), 635 (sh), 604 (sh), 582 (m), 545 (w), 427 (m).

References

1. N. V. Gerbeleu, A. S. Batsanov, G. A. Timko, Y. T. Struchkov, K. M. Indrichan, G. A. Popovich, *Dokl. Akad. Nauk SSSR (Russ.)*, 1987, **293**, 364.
2. G. M. Sheldrick, SHELXS-97 and SHELXL-97, University of Göttingen, Germany, 2003.
3. G. M. Sheldrick, CELL_NOW, University of Göttingen, Germany, 2008.
4. G. M. Sheldrick, TWINABS, University of Göttingen, Germany, 2008.

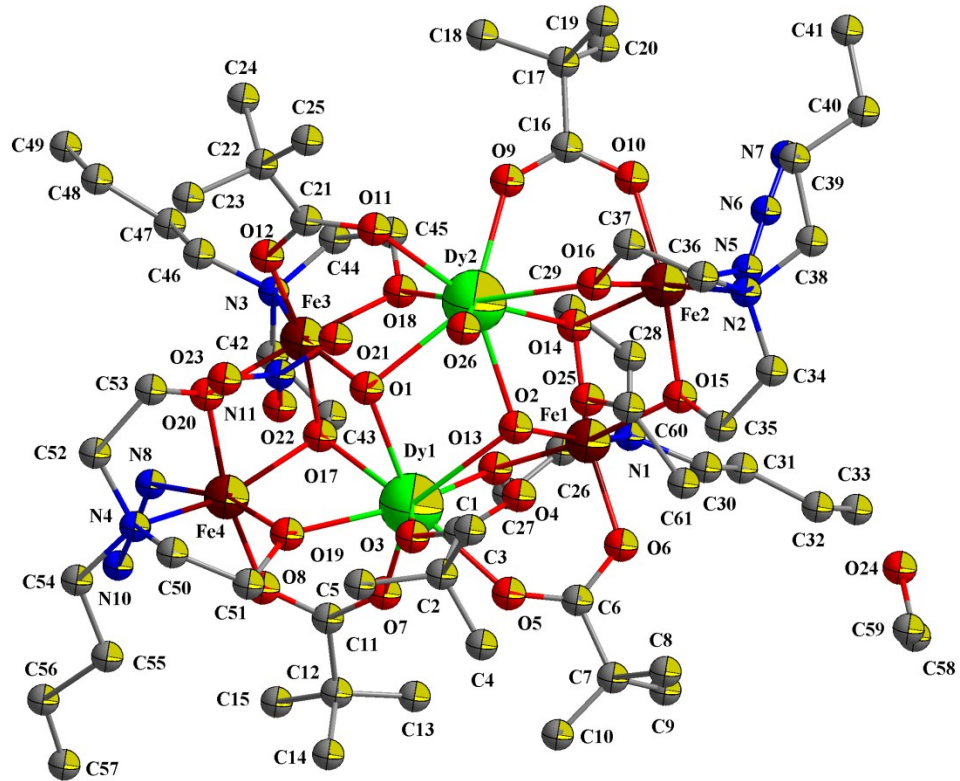


Figure S1. The molecular structure of $[Fe_4Dy_2(OH)_2(N_3)_2(bdea)_4(O_2CCMe_3)_5(H_2O)]NO_3 \cdot 2(EtOH)$ (1) with numbering scheme. Hydrogen and disorder atoms are omitted for clarity.

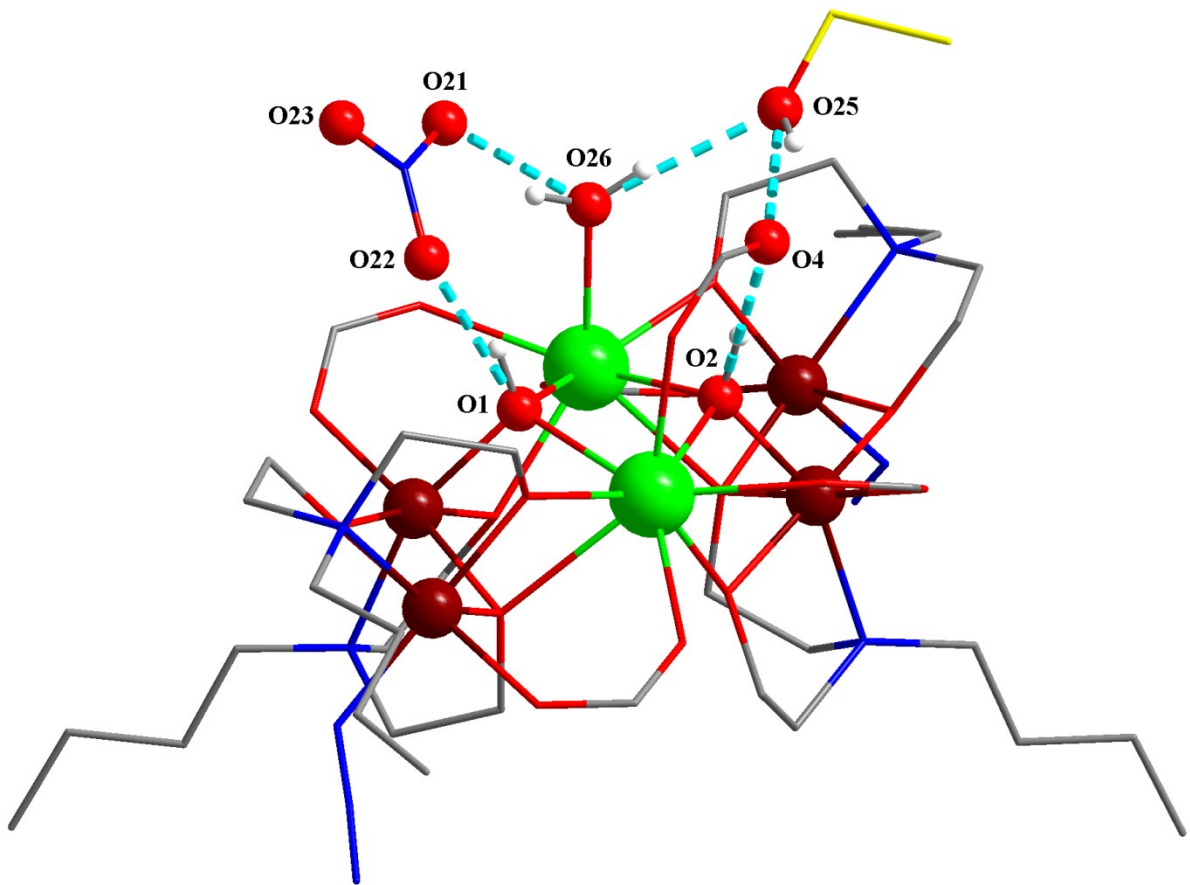


Figure S2. A view of hydrogen bond interactions in **1**. *tert*-Butyl groups of pivalates and hydrogen atoms (except those that form hydrogen bonds) are omitted for clarity. Hydrogen bonds are shown as blue dotted lines. Color scheme: Dy, green spheres; Fe, brown spheres; O, red sticks; O atoms that participate in the formation of hydrogen bonds are shown as red balls; N, blue sticks; C, grey sticks; C atoms of solvate ethanol are highlighted in yellow. The coordinated water molecule hydrogen-binds to nitrate [O26···O21, 2.686(9) Å] and solvate ethanol [O26···O25, 2.816(15) Å]. EtOH furthermore binds strongly [2.468(16) Å] to the carboxylate O4. Finally, the third nitrate oxygen site hydrogen-binds to a disordered solvate EtOH molecule [O23···O24, 2.736(13) Å].

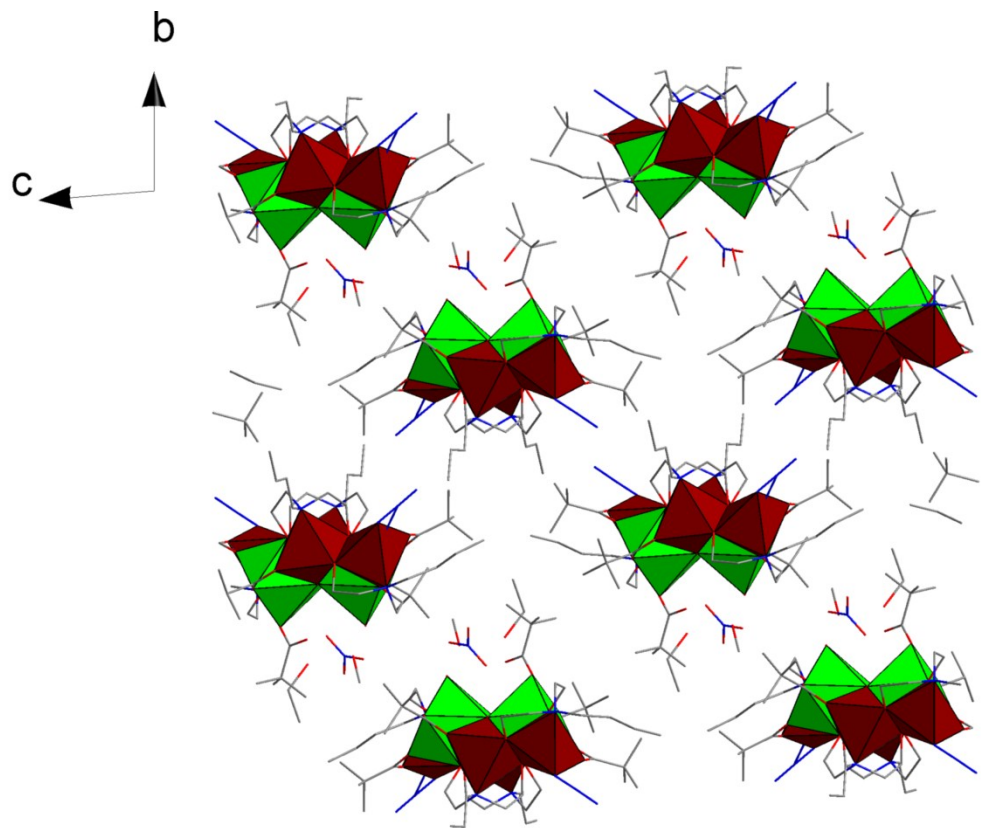


Figure S3. Packing diagram for **1**, a view along the a axis. Color scheme: Dy, green polyhedra; Fe, brown polyhedra; O, red sticks; N, blue sticks; C, grey sticks. Hydrogen atoms are omitted for clarity.

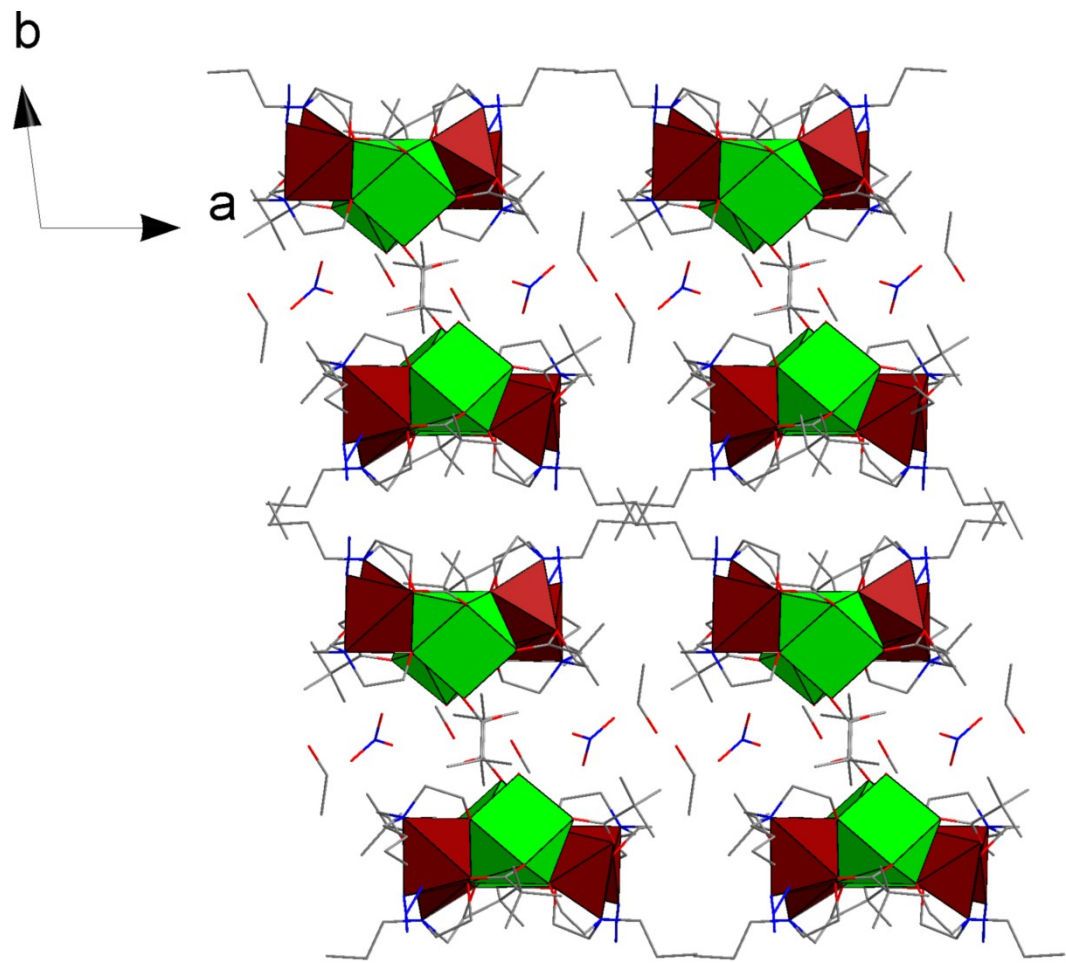


Figure S4. Packing diagram for **1**, a view along the *c* axis. Color scheme: Dy, green polyhedra; Fe, brown polyhedra; O, red sticks; N, blue sticks; C, grey sticks. Hydrogen atoms are omitted for clarity.

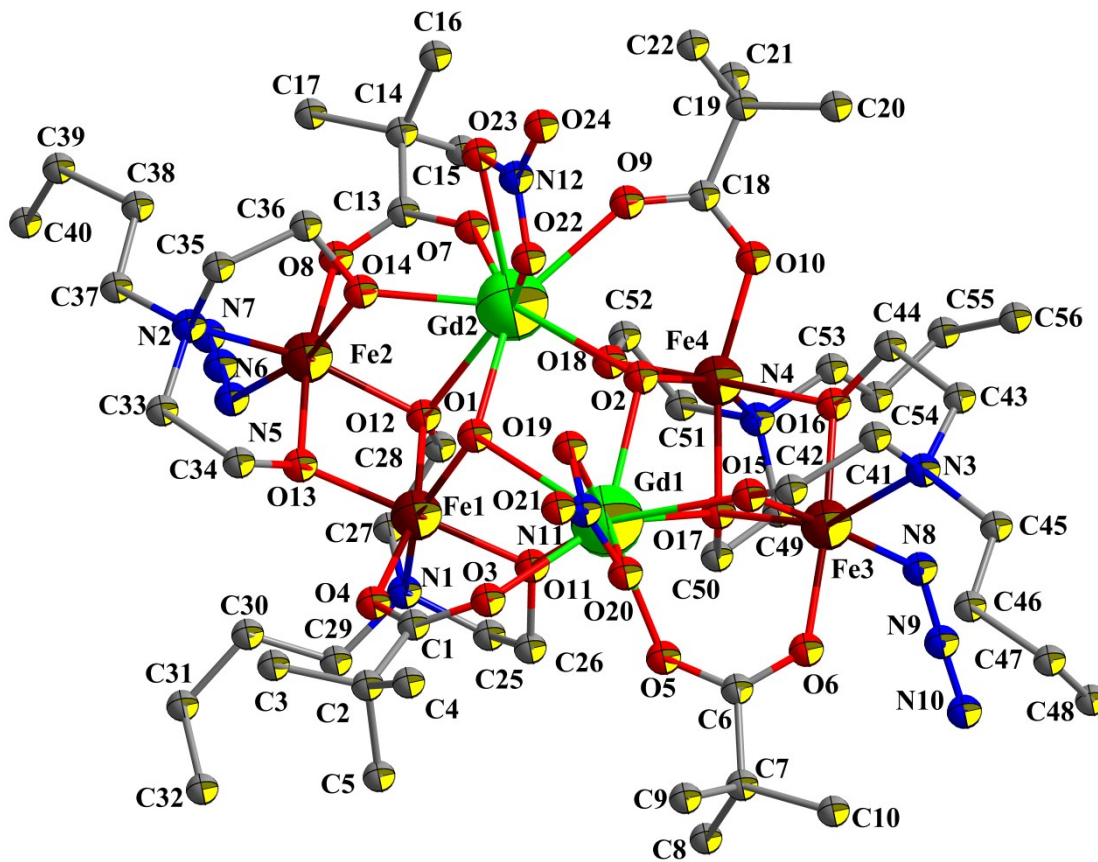


Figure S5. The molecular structure of $[\text{Fe}_4\text{Gd}_2(\text{OH})_2(\text{N}_3)_2(\text{bdea})_4(\text{O}_2\text{CCMe}_3)_4(\text{NO}_3)_2]\cdot 3(\text{EtOH})$ (**3**) with numbering scheme. Hydrogen atoms and solvent ethanol molecules are omitted for clarity.

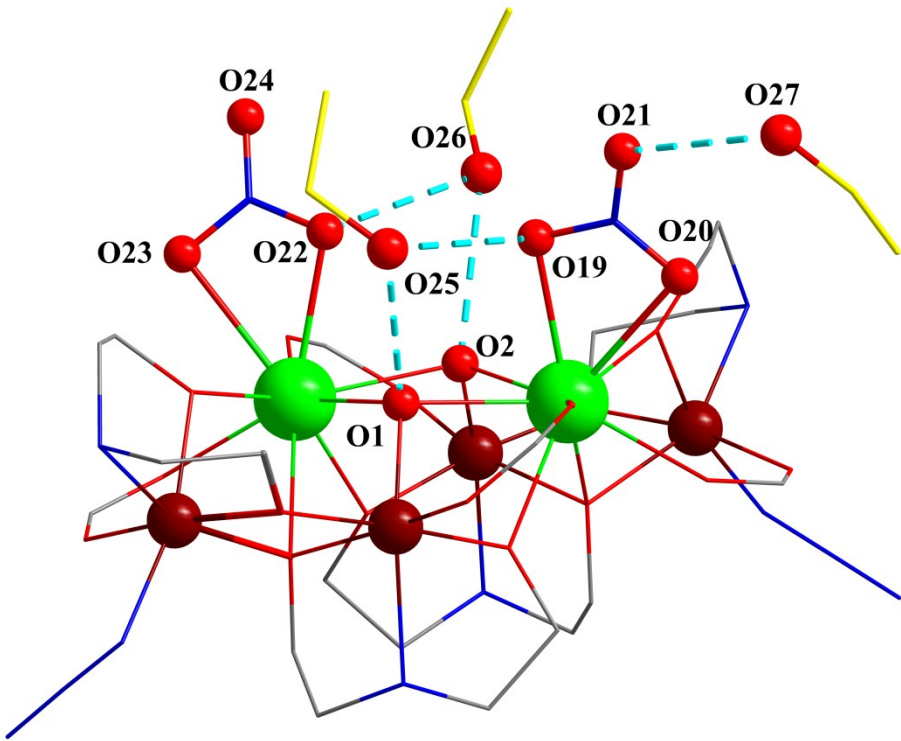


Figure S6. A view of hydrogen bond interactions in **3**. *tert*-Butyl groups of pivalates, butyl groups of N-butyldiethanolamine and hydrogen atoms are omitted for clarity. Hydrogen bonds are shown as blue dotted lines. Color scheme: Gd, green spheres; Fe, brown spheres; O, red sticks; O atoms that participate in the formation of hydrogen bonds are shown as red balls; N, blue sticks; C, grey sticks; C atoms of solvate ethanol are highlighted in yellow. Three solvate EtOH molecules form intermolecular O···O hydrogen bonds with OH⁻ groups [2.802(11)/2.804(11) Å] as well as with the coordinated nitrate anions [2.812(12)–2.984(2) Å].

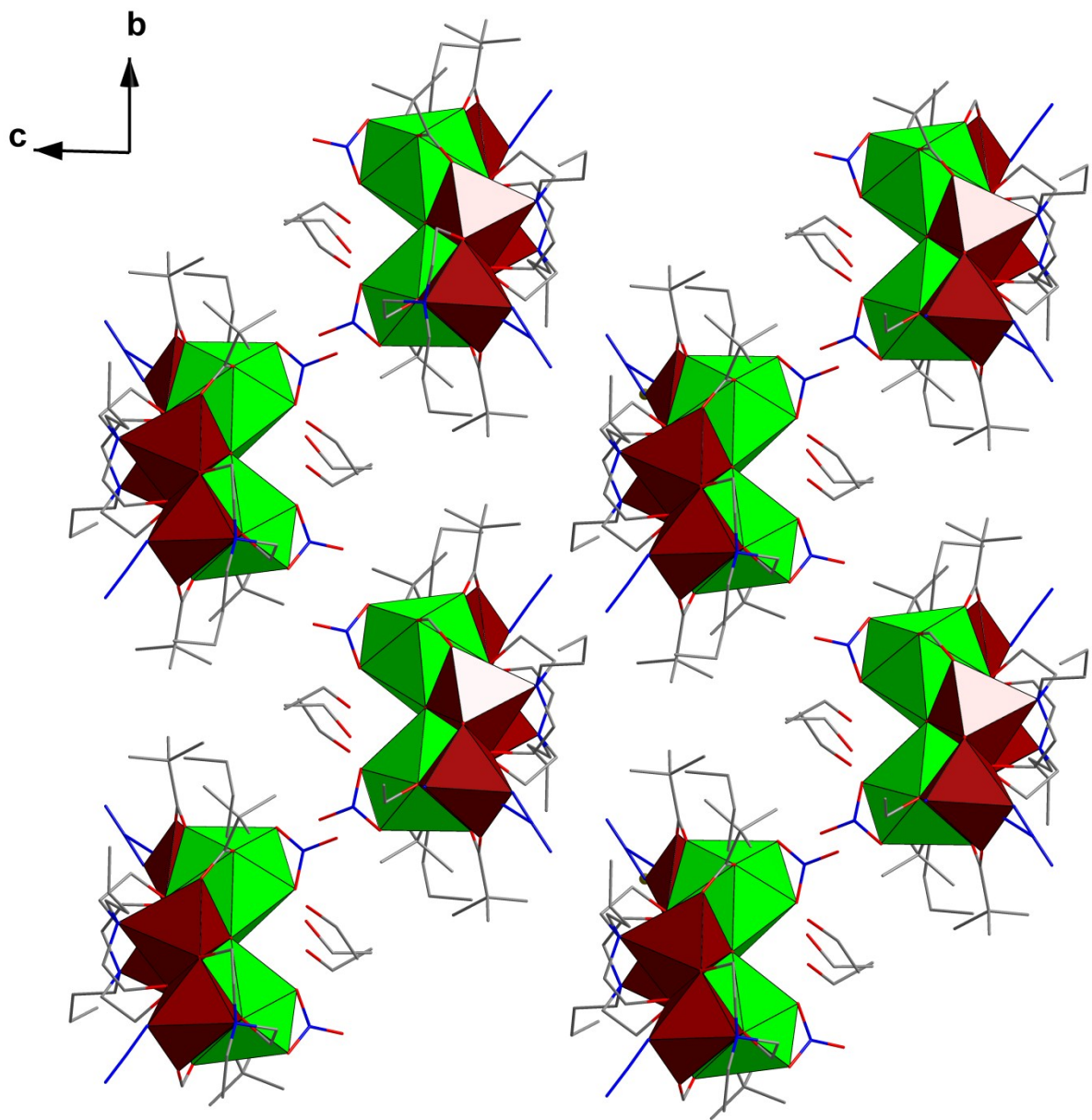


Figure S7. Packing diagram for **3**, a view along the a axis. Color scheme: Gd, green polyhedra; Fe, brown polyhedra; O, red sticks; N, blue sticks; C, grey sticks. Hydrogen atoms are omitted for clarity.

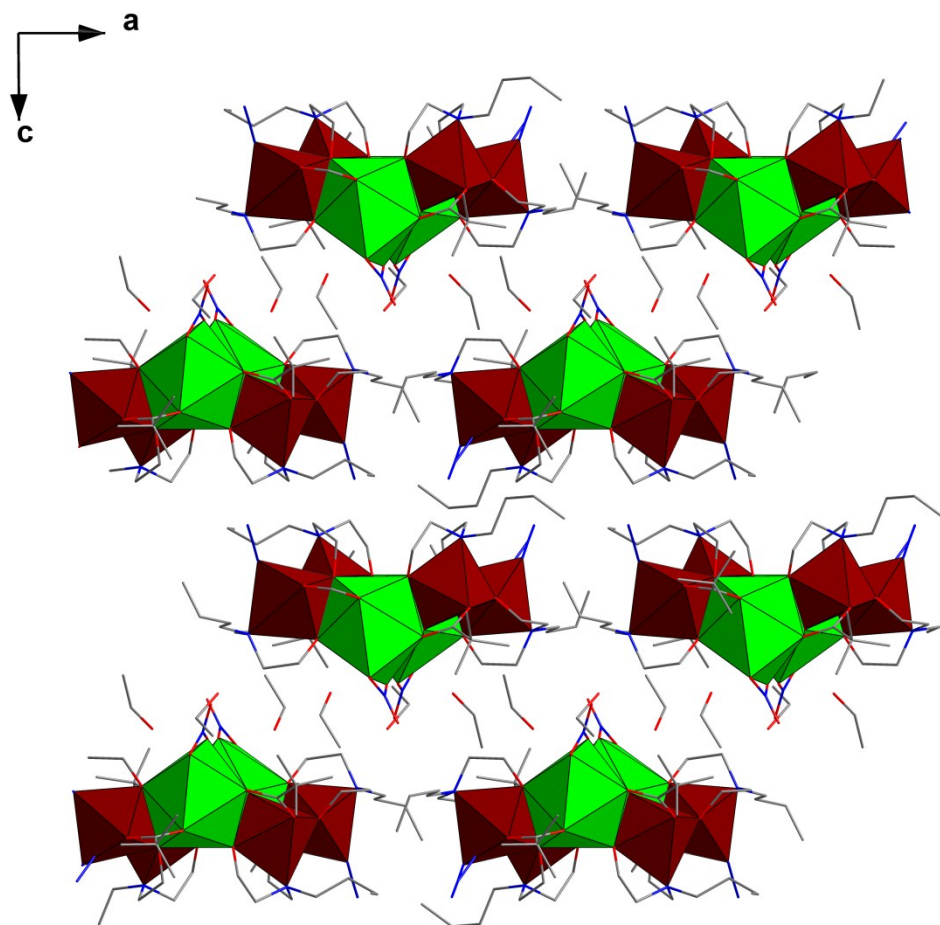


Figure S8. Packing diagram for **3**, a view along the *b* axis. Color scheme: Gd, green polyhedra; Fe, brown polyhedra; O, red sticks; N, blue sticks; C, grey sticks. Hydrogen atoms are omitted for clarity.

Table S1. Crystal data and details of structural determinations for **1–4**

	1, {Fe₄Dy₂}	2, {Fe₄Y₂}	3, {Fe₄Gd₂}	4, {Fe₄Eu₂}
Empirical formula	C ₆₁ H ₁₂₉ Dy ₂ Fe ₄ N ₁₁ O ₂₆	C ₆₁ H ₁₂₉ Fe ₄ N ₁₁ O ₂₆ Y ₂	C ₅₈ H ₁₂₄ Fe ₄ Gd ₂ N ₁₂ O ₂₇	C ₅₈ H ₁₂₄ Eu ₂ Fe ₄ N ₁₂ O ₂₇
<i>M_r</i> / g mol ⁻¹	1981.15	1833.97	1959.59	1949.01
<i>T</i> / K	100(2)	100(2)	100(2)	100(2)
Wavelength / Å	0.71073	0.71073	0.71073	0.71073
Crystal system	Triclinic	Triclinic	Triclinic	Triclinic
Space group	<i>P</i> -1	<i>P</i> -1	<i>P</i> -1	<i>P</i> -1
Unit cell dimensions				
<i>a</i> / Å	14.4435(9)	14.423(4)	15.278(2)	15.269(2)
<i>b</i> / Å	17.3551(11)	17.383(5)	16.228(3)	16.216(2)
<i>c</i> / Å	18.0251(12)	18.109(5)	16.672(3)	16.655(2)
α / °	92.765(2)	92.839(7)	88.375(2)	88.379(2)
β / °	104.869(2)	104.682(7)	89.375(2)	89.398(2)
γ / °	96.595(2)	96.704(7)	82.960(2)	82.993(2)
<i>V</i> / Å ³	4323.9(5)	4347(2)	4100.6(11)	4091.3(9)
<i>Z</i> , ρ / Mg m ⁻³	2, 1.522	2, 1.401	2, 1.587	2, 1.582
μ / mm ⁻¹	2.433	2.043	2.361	2.279
<i>F</i> (000)	2032	1924	2008	2004
Crystal size / mm ³	0.37 × 0.08 × 0.08	0.45 × 0.15 × 0.11	0.35 × 0.33 × 0.26	0.34 × 0.31 × 0.24
θ range for data collection	2.01 – 24.47	1.62 – 23.58	1.26 – 25.26	1.27 – 27.15
Index ranges	$-16 \leq h \leq 16$, $-20 \leq k \leq 20$, $-20 \leq l \leq 20$	$-15 \leq h \leq 16$, $-19 \leq k \leq 19$, $-18 \leq l \leq 20$	$-18 \leq h \leq 18$, $-19 \leq k \leq 19$, $0 \leq l \leq 19$	$-19 \leq h \leq 19$, $-20 \leq k \leq 20$, $0 \leq l \leq 21$
Reflections collected	44844	30990	31637	32597
Independent reflections	14285 [$R_{\text{int}} = 0.0658$]	12821 [$R_{\text{int}} = 0.0897$]	16127 [$R_{\text{int}} = 0.0836$]	17568 [$R_{\text{int}} = 0.0681$]
Completeness to θ_{max}	99.6%	98.6 %	97.0%	96.8 %
Data / restraints / parameters	14285 / 507 / 1040	12821 / 369 / 924	16127 / 474 / 944	17568 / 474 / 947
Goodness-of-fit on F^2	1.028	1.028	1.032	1.027
Final <i>R</i> indices [$I > 2\sigma(I)$]: <i>R</i> ₁ , <i>wR</i> ₂	0.0548, 0.1246	0.0725, 0.1719	0.0660, 0.1677	0.0474, 0.1124
<i>R</i> indices (all data): <i>R</i> ₁ , <i>wR</i> ₂	0.0746, 0.1370	0.1165, 0.1896	0.0750, 0.1734	0.0579, 0.1170
Largest diff. peak, hole (e Å ⁻³)	1.343, -1.380	1.418, -1.218	3.652, -2.409	2.124, -1.790

Table S2. Selected bond distances (Å) and angles (°) in **1**

Dy1–O19	2.294(5)	Dy2–O18	2.290(5)
Dy1–O13	2.304(5)	Dy2–O16	2.291(5)
Dy1–O3	2.305(4)	Dy2–O9	2.334(5)
Dy1–O7	2.313(5)	Dy2–O11	2.335(5)
Dy1–O5	2.348(5)	Dy2–O2	2.352(5)
Dy1–O1	2.378(5)	Dy2–O26	2.364(5)
Dy1–O2	2.435(5)	Dy2–O1	2.447(5)
Dy1–O17	2.597(5)	Dy2–O14	2.574(5)
Fe1–O2	1.943(5)	Fe3–O12	1.953(6)
Fe1–O15	1.967(6)	Fe3–O20	1.966(6)
Fe1–O6	1.968(5)	Fe3–O1	1.969(5)
Fe1–O13	1.985(5)	Fe3–O18	1.985(5)

Fe1–O14	2.076(6)	Fe3–O17	2.069(5)
Fe1–N1	2.218(7)	Fe3–N3	2.196(7)
Fe2–O16	1.976(6)	Fe4–O19	1.949(5)
Fe2–N5	1.992(8)	Fe4–N8	1.990(8)
Fe2–O15	2.000(6)	Fe4–O20	2.018(5)
Fe2–O10	2.027(6)	Fe4–O17	2.045(5)
Fe2–O14	2.055(5)	Fe4–O8	2.046(6)
Fe2–N2	2.212(7)	Fe4–N4	2.215(6)
Metal···metal distances			
Dy1···Fe1	3.3915(12)	Dy2···Fe3	3.4041(11)
Dy1···Fe3	3.5415(12)	Dy2···Fe2	3.4508(12)
Dy1···Fe4	3.4700(12)	Dy2···Fe1	3.5318(12)
Dy1···Dy2	3.8711(6)		
O19–Dy1–O3	78.55(18)	O18–Dy2–O16	144.00(18)
O19–Dy1–O13	142.69(17)	O18–Dy2–O9	79.68(19)
O3–Dy1–O13	138.71(18)	O16–Dy2–O9	75.59(19)
O19–Dy1–O7	76.16(18)	O18–Dy2–O11	79.01(19)
O3–Dy1–O7	121.53(19)	O16–Dy2–O11	120.1(2)
O13–Dy1–O7	79.49(18)	O9–Dy2–O11	78.3(2)
O19–Dy1–O5	122.8(2)	O18–Dy2–O2	103.11(18)
O3–Dy1–O5	74.78(19)	O16–Dy2–O2	81.53(18)
O13–Dy1–O5	77.17(18)	O9–Dy2–O2	141.47(19)
O7–Dy1–O5	76.5(2)	O11–Dy2–O2	140.19(18)
O19–Dy1–O1	79.64(17)	O18–Dy2–O26	140.0(19)
O3–Dy1–O1	82.14(18)	O16–Dy2–O26	75.8(2)
O13–Dy1–O1	103.36(17)	O9–Dy2–O26	120.3(2)
O7–Dy1–O1	141.01(18)	O11–Dy2–O26	72.79(19)
O5–Dy1–O1	142.46(18)	O2–Dy2–O26	82.38(18)
O19–Dy1–O2	143.68(17)	O18–Dy2–O1	66.19(17)
O3–Dy1–O2	79.15(17)	O16–Dy2–O1	144.01(17)
O13–Dy1–O2	65.58(16)	O9–Dy2–O1	140.23(18)
O7–Dy1–O2	140.16(17)	O11–Dy2–O1	75.75(18)
O5–Dy1–O2	77.58(19)	O2–Dy2–O1	69.41(16)
O1–Dy1–O2	69.18(17)	O26–Dy2–O1	79.60(18)
O19–Dy1–O17	66.80(17)	O18–Dy2–O14	80.46(17)
O3–Dy1–O17	136.61(17)	O16–Dy2–O14	68.58(18)
O13–Dy1–O17	80.03(16)	O9–Dy2–O14	76.2(2)
O7–Dy1–O17	75.43(18)	O11–Dy2–O14	149.69(18)
O5–Dy1–O17	146.46(17)	O2–Dy2–O14	66.61(17)
O1–Dy1–O17	67.05(16)	O26–Dy2–O14	135.23(18)
O2–Dy1–O17	114.42(17)	O1–Dy2–O14	115.35(17)
O2–Fe1–O15	101.9(2)	O12–Fe3–O20	92.6(2)
O2–Fe1–O6	100.1(2)	O12–Fe3–O1	97.0(2)
O15–Fe1–O6	93.0(2)	O20–Fe3–O1	102.9(2)
O2–Fe1–O13	81.70(19)	O12–Fe3–O18	95.7(2)
O15–Fe1–O13	169.3(2)	O20–Fe3–O18	169.9(2)
O6–Fe1–O13	96.3(2)	O1–Fe3–O18	81.8(2)
O2–Fe1–O14	84.8(2)	O12–Fe3–O17	169.0(2)
O15–Fe1–O14	76.3 (2)	O20–Fe3–O17	76.4(2)
O6–Fe1–O14	169.0(2)	O1–Fe3–O17	86.0(2)
O13–Fe1–O14	94.2(2)	O18–Fe3–O17	95.2(2)

O2–Fe1–N1	155.9(2)	O12–Fe3–N3	98.4(3)
O15–Fe1–N1	95.7(2)	O20–Fe3–N3	93.6(2)
O6–Fe1–N1	95.4(3)	O1–Fe3–N3	156.9(2)
O13–Fe1–N1	78.2(2)	O18–Fe3–N3	79.6(2)
O14–Fe1–N1	83.4(2)	O17–Fe3–N3	82.2(3)
O16–Fe2–N5	167.0(3)	O19–Fe4–N8	165.0(3)
O16–Fe2–O15	96.0(2)	O19–Fe4–O20	95.5(2)
N5–Fe2–O15	91.7(3)	N8–Fe4–O20	94.1(3)
O16–Fe2–O10	88.1(2)	O19–Fe4–O8	88.2(2)
N5–Fe2–O10	87.0(3)	N8–Fe4–O8	85.0(3)
O15–Fe2–O10	165.6(3)	O20–Fe4–O8	166.9(2)
O16–Fe2–O14	86.0(2)	O19–Fe4–O17	85.2(2)
N5–Fe2–O14	106.0(3)	N8–Fe4–O17	108.4(3)
O15–Fe2–O14	76.1(2)	O20–Fe4–O17	75.9(2)
O10–Fe2–O14	90.5(2)	O8–Fe4–O17	92.0(2)
O16–Fe2–N2	80.1(2)	O19–Fe4–N4	81.0(2)
N5–Fe2–N2	90.8(3)	N8–Fe4–N4	89.3(3)
O15–Fe2–N2	81.7(2)	O20–Fe4–N4	80.4(2)
O10–Fe2–N2	112.6(3)	O8–Fe4–N4	112.6(2)
O14–Fe2–N2	152.4(2)	O17–Fe4–N4	151.2(2)

Table S3. Hydrogen bonds for **1** (Å and °)

D–H···A	d(D–H)	d(H···A)	d(D···A)	∠(DHA)
O1–H1A···O22	0.96	1.85	2.777(8)	163.5
O2–H2A···O4	0.98	1.63	2.608(8)	172.6
O24–H24···O23 ^{#1}	0.84	1.97	2.736(13)	150.7
O25–H25···O4	0.84	1.71	2.468(16)	149.2
O25'–H25'···O24	0.84	1.65	2.49(3)	170.2
O26–H26C···O21	0.84	1.90	2.686(9)	155.8
O26–H26D···O25	0.84	1.99	2.816(15)	171.3

Symmetry transformations used to generate equivalent atoms: #1 $x-1, y, z$

Table S4. Selected bond distances (Å) and angles (°) in **2**

Y1–O3	2.291(5)	Y2–O16	2.285(5)
Y1–O19	2.294(5)	Y2–O17	2.294(5)
Y1–O13	2.298(5)	Y2–O9	2.313(5)
Y1–O5	2.304(5)	Y2–O11	2.320(6)
Y1–O7	2.331(5)	Y2–O26	2.334(5)
Y1–O1	2.361(5)	Y2–O2	2.343(5)
Y1–O2	2.433(5)	Y2–O1	2.447(5)
Y1–O18	2.600(5)	Y2–O14	2.566(5)
Fe1–O2	1.944(5)	Fe3–O12	1.961(5)
Fe1–O8	1.979(6)	Fe3–O1	1.971(5)
Fe1–O15	1.984(5)	Fe3–O20	1.976(5)

Fe1–O13	1.989(5)	Fe3–O17	1.993(5)
Fe1–O14	2.089(5)	Fe3–O18	2.075(5)
Fe1–N1	2.202(7)	Fe3–N3	2.209(7)
Fe2–O16	1.968(6)	Fe4–O19	1.957(5)
Fe2–N5	1.997(8)	Fe4–N8	1.988(7)
Fe2–O15	2.000(6)	Fe4–O20	2.011(5)
Fe2–O10	2.036(6)	Fe4–O6	2.043(6)
Fe2–O14	2.063(5)	Fe4–O18	2.046(5)
Fe2–N2	2.223(7)	Fe4–N4	2.212(7)
Metal···metal distances			
Y1···Fe1	3.3878(15)	Y2···Fe3	3.4033(15)
Y1···Fe3	3.5448(15)	Y2···Fe1	3.5239(16)
Y1···Fe4	3.4734(15)	Y2···Fe2	3.4477(16)
Y2···Y1	3.8712(16)		
O3–Y1–O19	78.30(18)	O16–Y2–O17	143.54(19)
O3–Y1–O13	138.98(18)	O16–Y2–O9	75.89(19)
O19–Y1–O13	142.70(17)	O17–Y2–O9	79.45(18)
O3–Y1–O5	121.2(2)	O16–Y2–O11	120.46(19)
O19–Y1–O5	76.35(18)	O17–Y2–O11	78.99(18)
O13–Y1–O5	79.73(18)	O9–Y2–O11	77.6(2)
O3–Y1–O7	75.03 (19)	O16–Y2–O26	75.82(19)
O19–Y1–O7	122.87(19)	O17–Y2–O26	140.46(19)
O13–Y1–O7	77.35(19)	O9–Y2–O26	120.0(2)
O5–Y1–O7	76.06(19)	O11–Y2–O26	73.16(19)
O3–Y1–O1	82.22(18)	O16–Y2–O2	81.48(18)
O19–Y1–O1	79.43(17)	O17–Y2–O2	103.22(17)
O13–Y1–O1	103.08(17)	O9–Y2–O2	142.29(19)
O5–Y1–O1	141.11(18)	O11–Y2–O2	140.06(18)
O7–Y1–O1	142.77(18)	O26–Y2–O2	82.06(18)
O3–Y1–O2	79.12(18)	O16–Y2–O1	143.94(18)
O19–Y1–O2	143.19(17)	O17–Y2–O1	66.41(17)
O13–Y1–O2	65.80(16)	O9–Y2–O1	140.02(17)
O5–Y1–O2	140.45(18)	O11–Y2–O1	76.00(17)
O7–Y1–O2	77.93(19)	O26–Y2–O1	79.84(17)
O1–Y1–O2	69.00(16)	O2–Y2–O1	69.04(16)
O3–Y1–O18	136.53(17)	O16–Y2–O14	68.60(19)
O19–Y1–O18	66.85(17)	O17–Y2–O14	79.90(17)
O13–Y1–O18	79.79(16)	O9–Y2–O14	76.6(2)
O5–Y1–O18	75.66(18)	O11–Y2–O14	149.20(18)
O7–Y1–O18	146.24(17)	O26–Y2–O14	135.38(17)
O1–Y1–O18	66.96(16)	O2–Y2–O14	67.10(17)
O2–Y1–O18	114.38(17)	O1–Y2–O14	115.05(17)
O2–Fe1–O8	99.9(2)	O12–Fe3–O1	97.8(2)
O2–Fe1–O15	101.8(2)	O12–Fe3–O20	93.0(2)
O8–Fe1–O15	92.8(2)	O1–Fe3–O20	102.7(2)
O2–Fe1–O13	81.7(2)	O12–Fe3–O17	95.4(2)
O8–Fe1–O13	96.1(2)	O1–Fe3–O17	82.0(2)
O15–Fe1–O13	169.8(2)	O20–Fe3–O17	169.7(2)
O2–Fe1–O14	84.7(2)	O12–Fe3–O18	168.8(2)
O8–Fe1–O14	168.9(2)	O1–Fe3–O18	85.39(19)
O15–Fe1–O14	76.4(2)	O20–Fe3–O18	75.8(2)

O13–Fe1–O14	94.6(2)	O17–Fe3–O18	95.7(2)
O2–Fe1–N1	155.8(3)	O12–Fe3–N3	99.1(3)
O8–Fe1–N1	97.1(3)	O1–Fe3–N3	156.1(2)
O15–Fe1–N1	94.4(2)	O20–Fe3–N3	93.0(2)
O13–Fe1–N1	79.5(2)	O17–Fe3–N3	79.8(2)
O14–Fe1–N1	81.7(3)	O18–Fe3–N3	81.2(3)
O16–Fe2–N5	167.1(3)	O19–Fe4–N8	165.0(3)
O16–Fe2–O15	95.8(2)	O19–Fe4–O20	95.2(2)
N5–Fe2–O15	91.9(3)	N8–Fe4–O20	93.9(3)
O16–Fe2–O10	88.4(3)	O19–Fe4–O6	88.7(2)
N5–Fe2–O10	86.7(3)	N8–Fe4–O6	85.1(3)
O15–Fe2–O10	165.6(2)	O20–Fe4–O6	166.6(2)
O16–Fe2–O14	85.8(2)	O19–Fe4–O18	85.1(2)
N5–Fe2–O14	106.2(3)	N8–Fe4–O18	108.7(3)
O15–Fe2–O14	76.6(2)	O20–Fe4–O18	75.6(2)
O10–Fe2–O14	90.1(2)	O6–Fe4–O18	91.9(2)
O16–Fe2–N2	80.4(2)	O19–Fe4–N4	80.8(2)
N5–Fe2–N2	90.5(3)	N8–Fe4–N4	89.1(3)
O15–Fe2–N2	81.4(2)	O20–Fe4–N4	80.5(2)
O10–Fe2–N2	112.9(2)	O6–Fe4–N4	112.9(2)
O14–Fe2–N2	152.6(2)	O18–Fe4–N4	151.0(2)

Table S5. Hydrogen bonds for **2** [Å and °]

D–H···A	d(D–H)	d(H···A)	d(D···A)	∠(DHA)
O1–H1···O21 ^{#1}	0.90	1.93	2.803(8)	163.0
O2–H2···O4	0.90	1.73	2.601(8)	162.6
O26–H26D···O23 ^{#1}	0.90	1.80	2.701(9)	174.0

Symmetry transformations used to generate equivalent atoms: #1 $x, -1+y, z$

* Two solvate ethanol molecules were removed by the SQUEEZE routine.

Table S6. Selected bond distances (Å) and angles (°) in **3**

Gd1–O5	2.318(8)	Gd2–O7	2.331(7)
Gd1–O11	2.334(7)	Gd2–O18	2.362(7)
Gd1–O15	2.356(7)	Gd2–O14	2.378(7)
Gd1–O3	2.389(8)	Gd2–O9	2.404(8)
Gd1–O2	2.401(7)	Gd2–O1	2.421(7)
Gd1–O19	2.482(7)	Gd2–O22	2.460(8)
Gd1–O1	2.514(7)	Gd2–O2	2.514(7)
Gd1–O17	2.626(6)	Gd2–O23	2.648(8)
Gd1–O20	2.642(7)	Gd2–O12	2.653(7)
Gd1–N11	2.959(8)	Gd2–N12	2.943(11)
Fe1–O13	1.971(7)	Fe3–O15	1.970(7)
Fe1–O11	1.974(7)	Fe3–N8	1.997(8)

Fe1–O1	1.977(7)	Fe3–O16	2.019(7)
Fe1–O4	1.988(7)	Fe3–O6	2.024(8)
Fe1–O12	2.065(5)	Fe3–O17	2.064(7)
Fe1–N1	2.253(9)	Fe3–N3	2.205(9)
Fe2–O14	1.965(7)	Fe4–O18	1.966(7)
Fe2–O13	2.015(7)	Fe4–O2	1.986(6)
Fe2–N5	2.012(9)	Fe4–O16	1.990(7)
Fe2–O8	2.041(7)	Fe4–O10	1.992(8)
Fe2–O12	2.058(7)	Fe4–O17	2.081(7)
Fe2–N2	2.226(9)	Fe4–N4	2.207(8)
Metal···metal distances			
Gd1···Fe1	3.4700(16)	Gd2···Fe4	3.4687(15)
Gd1···Fe3	3.5127(15)	Gd2···Fe2	3.5047(16)
Gd1···Fe4	3.5968(15)	Gd2···Fe1	3.6030(16)
Gd1···Gd2	4.0534(10)		
O5–Gd1–O11	81.0(3)	O7–Gd2–O18	80.2(2)
O5–Gd1–O15	79.9(3)	O7–Gd2–O14	77.6(2)
O11–Gd1–O15	139.6(2)	O18–Gd2–O14	138.4(2)
O5–Gd1–O3	81.4(3)	O7–Gd2–O9	80.0(3)
O11–Gd1–O3	75.0(3)	O18–Gd2–O9	75.3(2)
O15–Gd1–O3	135.8(3)	O14–Gd2–O9	133.2(2)
O5–Gd1–O2	138.7(3)	O7–Gd2–O1	139.7(3)
O11–Gd1–O2	99.0(2)	O18–Gd2–O1	98.8(2)
O15–Gd1–O2	73.7(2)	O14–Gd2–O1	77.3(2)
O3–Gd1–O2	139.0(3)	O9–Gd2–O1	139.3(2)
O5–Gd1–O19	125.8(3)	O7–Gd2–O22	130.5(3)
O11–Gd1–O19	135.7(2)	O18–Gd2–O22	132.3(2)
O15–Gd1–O19	83.7(2)	O14–Gd2–O22	88.3(2)
O3–Gd1–O19	75.5(3)	O9–Gd2–O22	76.1(3)
O2–Gd1–O19	82.6(2)	O1–Gd2–O22	79.5(3)
O5–Gd1–O1	141.3(3)	O7–Gd2–O2	140.3(2)
O11–Gd1–O1	64.7(2)	O18–Gd2–O2	64.9(2)
O15–Gd1–O1	138.2(2)	O14–Gd2–O2	141.7(2)
O3–Gd1–O1	73.0(2)	O9–Gd2–O2	73.6(2)
O2–Gd1–O1	68.1(2)	O1–Gd2–O2	67.8(2)
O19–Gd1–O1	75.4(2)	O22–Gd2–O2	70.8(2)
O5–Gd1–O17	74.4(3)	O7–Gd2–O23	80.7(3)
O11–Gd1–O17	74.8(2)	O18–Gd2–O23	137.9(2)
O15–Gd1–O17	65.9(2)	O14–Gd2–O23	71.5(2)
O3–Gd1–O17	143.7(2)	O9–Gd2–O23	64.6(2)
O2–Gd1–O17	66.0(2)	O1–Gd2–O23	119.7(2)
O19–Gd1–O17	140.8(3)	O22–Gd2–O23	49.9(3)
O1–Gd1–O17	110.9(2)	O2–Gd2–O23	112.5(2)
O5–Gd1–O20	75.8(3)	O7–Gd2–O12	75.8(2)
O11–Gd1–O20	136.6(2)	O18–Gd2–O12	74.0(2)
O15–Gd1–O20	71.0(2)	O14–Gd2–O12	66.8(2)
O3–Gd1–O20	65.7(3)	O9–Gd2–O12	143.5(2)
O2–Gd1–O20	122.6(2)	O1–Gd2–O12	65.4(2)
O19–Gd1–O20	50.1(2)	O22–Gd2–O12	140.2(2)
O1–Gd1–O20	116.9(2)	O2–Gd2–O12	109.7(2)
O17–Gd1–O20	130.8(2)	O23–Gd2–O12	135.5(2)
O5–Gd1–N11	100.4(3)	O7–Gd2–N12	104.9(3)

O11–Gd1–N11	139.4(2)	O18–Gd2–N12	136.8(3)
O15–Gd1–N11	79.2(2)	O14–Gd2–N12	83.1(3)
O3–Gd1–N11	65.3(3)	O9–Gd2–N12	63.9(3)
O2–Gd1–N11	105.2(2)	O1–Gd2–N12	102.8(3)
O19–Gd1–N11	25.5(3)	O22–Gd2–N12	25.7(3)
O1–Gd1–N11	94.8(2)	O2–Gd2–N12	89.5(2)
O17–Gd1–N11	145.1(2)	O23–Gd2–N12	25.0(3)
O20–Gd1–N11	25.0(2)	O12–Gd2–N12	149.2(2)
O13–Fe1–O11	177.1(3)	O15–Fe3–N8	166.4(3)
O13–Fe1–O1	100.0(3)	O15–Fe3–O16	95.4(3)
O11–Fe1–O1	82.3(3)	N8–Fe3–O16	93.8(3)
O13–Fe1–O4	87.5(3)	O15–Fe3–O6	87.9(3)
O11–Fe1–O4	93.8(3)	N8–Fe3–O6	84.9(3)
O1–Fe1–O4	100.7(3)	O16–Fe3–O6	169.6(3)
O13–Fe1–O12	76.4(3)	O15–Fe3–O17	84.7(3)
O11–Fe1–O12	102.2(3)	N8–Fe3–O17	107.4(3)
O1–Fe1–O12	85.8(3)	O16–Fe3–O17	75.6(3)
O4–Fe1–O12	163.5(3)	O6–Fe3–O17	94.9(3)
O13–Fe1–N1	98.1(3)	O15–Fe3–N3	81.7(3)
O11–Fe1–N1	79.2(3)	N8–Fe3–N3	89.9(3)
O1–Fe1–N1	154.4(3)	O16–Fe3–N3	80.4(3)
O4–Fe1–N1	98.1(3)	O6–Fe3–N3	109.9(3)
O12–Fe1–N1	80.9(3)	O17–Fe3–N3	151.1(3)
O14–Fe2–O13	93.1(3)	O18–Fe4–O2	83.0(3)
O14–Fe2–N5	165.6(3)	O18–Fe4–O16	171.7(3)
O13–Fe2–N5	96.3(3)	O2–Fe4–O16	104.9(3)
O14–Fe2–O8	87.6(3)	O18–Fe4–O10	94.1(3)
O13–Fe2–O8	168.8(3)	O2–Fe4–O10	100.6(3)
N5–Fe2–O8	85.3(3)	O16–Fe4–O10	86.8(3)
O14–Fe2–O12	87.3(3)	O18–Fe4–O17	103.0(3)
O13–Fe2–O12	75.6(3)	O2–Fe4–O17	84.8(3)
N5–Fe2–O12	105.6(3)	O16–Fe4–O17	75.9(3)
O8–Fe2–O12	93.3(3)	O10–Fe4–O17	162.6(3)
O14–Fe2–N2	81.7(3)	O18–Fe4–N4	79.7(3)
O13–Fe2–N2	81.6(3)	O2–Fe4–N4	155.4(3)
N5–Fe2–N2	88.9(3)	O16–Fe4–N4	92.1(3)
O8–Fe2–N2	109.6(3)	O10–Fe4–N4	97.9(3)
O12–Fe2–N2	154.0(3)	O17–Fe4–N4	82.3(3)

Table S7. Hydrogen bonds for **3** (Å and °)

D–H···A	d(D–H)	d(H···A)	d(D···A)	<(DHA)
O1–H1···O25	0.73	2.14	2.804(10)	151.0
O2–H2···O26	0.88	1.92	2.803(11)	179.7
O25–H25···O19	0.90	1.98	2.817(12)	153.9
O26–H26···O22	0.90	2.22	2.844(12)	126.0
O27–H27···O21	0.84	2.17	2.986(15)	163.4

Table S8. Selected bond distances (Å) and angles (°) in 4

Eu1–O5	2.331(5)	Eu2–O7	2.325(5)
Eu1–O11	2.346(4)	Eu2–O15	2.369(4)
Eu1–O18	2.362(4)	Eu2–O14	2.390(4)
Eu1–O3	2.397(5)	Eu2–O9	2.401(5)
Eu1–O2	2.418(4)	Eu2–O1	2.419(4)
Eu1–O19	2.488(5)	Eu2–O22	2.472(5)
Eu1–O1	2.523(4)	Eu2–O2	2.515(4)
Eu1–O16	2.634(4)	Eu2–O23	2.645(5)
Eu1–O20	2.632(5)	Eu2–O12	2.658(4)
Eu1–N11	2.978(6)	Eu2–N12	2.964(6)
Fe1–O11	1.976(4)	Fe3–O15	1.964(4)
Fe1–O13	1.979(4)	Fe3–O2	1.967(4)
Fe1–O4	1.981(5)	Fe3–O17	1.988(4)
Fe1–O1	1.984(4)	Fe3–O10	1.995(5)
Fe1–O12	2.070(4)	Fe3–O16	2.056(4)
Fe1–N1	2.255(5)	Fe3–N3	2.209(6)
Fe2–O14	1.962(4)	Fe4–O18	1.963(4)
Fe2–N5	2.002(5)	Fe4–N8	2.006(6)
Fe2–O13	2.009(4)	Fe4–O17	2.023(4)
Fe2–O12	2.037(4)	Fe4–O6	2.039(5)
Fe2–O8	2.043(5)	Fe4–O16	2.058(4)
Fe2–N2	2.217(5)	Fe4–N4	2.201(6)
Metal···metal distances			
Eu1···Fe1	3.4728(10)	Eu2···Fe3	3.4742(10)
Eu1···Fe4	3.5136(11)	Eu2···Fe2	3.5028(10)
Eu1···Fe3	3.6039(11)	Eu2···Fe1	3.6097(10)
Eu1···Eu2	4.0618(6)		
O5–Eu1–O11	81.13(16)	O7–Eu2–O15	80.05(15)
O5–Eu1–O18	79.93(16)	O7–Eu2–O14	77.53(15)
O11–Eu1–O18	139.16(15)	O15–Eu2–O14	138.40(14)
O5–Eu1–O3	81.65(16)	O7–Eu2–O9	80.31(16)
O11–Eu1–O3	75.18(16)	O15–Eu2–O9	75.24(15)
O18–Eu1–O3	136.27(15)	O14–Eu2–O9	133.39(14)
O5–Eu1–O2	137.97(16)	O7–Eu2–O1	139.40(16)
O11–Eu1–O2	98.27(14)	O15–Eu2–O1	98.98(15)
O18–Eu1–O2	73.50(15)	O14–Eu2–O1	77.12(15)
O3–Eu1–O2	139.25(15)	O9–Eu2–O1	139.21(15)
O5–Eu1–O19	126.03(17)	O7–Eu2–O22	130.52(16)
O11–Eu1–O19	135.68(16)	O15–Eu2–O22	131.90(15)
O18–Eu1–O19	84.01(15)	O14–Eu2–O22	88.75(15)
O3–Eu1–O19	75.56(17)	O9–Eu2–O22	75.51(16)
O2–Eu1–O19	83.17(15)	O1–Eu2–O22	79.86(16)
O5–Eu1–O1	141.55(15)	O7–Eu2–O2	139.74(15)
O11–Eu1–O1	64.86(14)	O15–Eu2–O2	64.31(14)
O18–Eu1–O1	137.88(14)	O14–Eu2–O2	142.16(14)
O3–Eu1–O1	73.06(15)	O9–Eu2–O2	73.28(14)
O2–Eu1–O1	68.04(13)	O1–Eu2–O2	68.17(13)
O19–Eu1–O1	75.18(15)	O22–Eu2–O2	71.14(14)
O5–Eu1–O16	74.67(15)	O7–Eu2–O23	81.27(16)
O11–Eu1–O16	74.83(14)	O15–Eu2–O23	138.02(16)

O18–Eu1–O16	65.39(14)	O14–Eu2–O23	71.68(15)
O3–Eu1–O16	144.10(15)	O9–Eu2–O23	64.73(15)
O2–Eu1–O16	64.89(13)	O1–Eu2–O23	119.28(16)
O19–Eu1–O16	140.33(16)	O22–Eu2–O23	49.41(16)
O1–Eu1–O16	110.60(14)	O2–Eu2–O23	112.64(14)
O5–Eu1–O20	76.42(16)	O7–Eu2–O12	75.41(15)
O11–Eu1–O20	136.96(15)	O15–Eu2–O12	74.32(14)
O18–Eu1–O20	71.62(15)	O14–Eu2–O12	66.36(14)
O3–Eu1–O20	65.62(15)	O9–Eu2–O12	143.71(14)
O2–Eu1–O20	122.85(14)	O1–Eu2–O12	65.53(14)
O19–Eu1–O20	49.64(15)	O22–Eu2–O12	140.59(15)
O1–Eu1–O20	116.44(14)	O2–Eu2–O12	109.82(13)
O16–Eu1–O20	131.32(14)	O23–Eu2–O12	135.28(14)
O5–Eu1–N11	100.63(17)	O7–Eu2–N12	105.28(18)
O11–Eu1–N11	139.50(15)	O15–Eu2–N12	136.62(16)
O18–Eu1–N11	79.73(15)	O14–Eu2–N12	83.38(15)
O3–Eu1–N11	65.24(16)	O9–Eu2–N12	63.78(17)
O2–Eu1–N11	105.84(15)	O1–Eu2–N12	102.69(17)
O19–Eu1–N11	25.52(16)	O22–Eu2–N12	25.30(17)
O1–Eu1–N11	94.59(15)	O2–Eu2–N12	89.80(15)
O20–Eu1–N11	24.54(14)	O23–Eu2–N12	24.84(16)
O16–Eu1–N11	145.12(14)	O12–Eu2–N12	149.06(15)
O11–Fe1–O13	176.53(19)	O15–Fe3–O2	82.91(17)
O11–Fe1–O4	93.80(19)	O15–Fe3–O17	172.08(19)
O13–Fe1–O4	88.22(19)	O2–Fe3–O17	104.77(18)
O11–Fe1–O1	82.68(18)	O15–Fe3–O10	93.66(18)
O13–Fe1–O1	99.71(18)	O2–Fe3–O10	100.90(18)
O4–Fe1–O1	100.98(19)	O17–Fe3–O10	86.86(19)
O11–Fe1–O12	102.21(18)	O15–Fe3–O16	103.38(18)
O13–Fe1–O12	75.58(18)	O2–Fe3–O16	84.92(17)
O4–Fe1–O12	163.39(19)	O17–Fe3–O16	75.78(18)
O1–Fe1–O12	85.60(17)	O10–Fe3–O16	162.59(19)
O11–Fe1–N1	78.96(19)	O15–Fe3–N3	79.47(19)
O13–Fe1–N1	97.99(19)	O2–Fe3–N3	155.12(19)
O4–Fe1–N1	97.5(2)	O17–Fe3–N3	92.63(19)
O1–Fe1–N1	154.7(2)	O10–Fe3–N3	97.6(2)
O12–Fe1–N1	81.45(18)	O16–Fe3–N3	82.26(19)
O14–Fe2–N5	165.3(2)	O18–Fe4–N8	166.8(2)
O14–Fe2–O13	93.07(19)	O18–Fe4–O17	94.94(18)
N5–Fe2–O13	95.8(2)	N8–Fe4–O17	93.5(2)
O14–Fe2–O12	87.74(18)	O18–Fe4–O6	88.37(19)
N5–Fe2–O12	105.8(2)	N8–Fe4–O6	85.1(2)
O13–Fe2–O12	75.66(18)	O17–Fe4–O6	169.72(19)
O14–Fe2–O8	88.01(19)	O18–Fe4–O16	84.66(17)
N5–Fe2–O8	85.5(2)	N8–Fe4–O16	107.4(2)
O13–Fe2–O8	169.03(19)	O17–Fe4–O16	74.99(17)
O12–Fe2–O8	93.49(18)	O6–Fe4–O16	95.69(18)
O14–Fe2–N2	81.02(19)	O18–Fe4–N4	81.58(19)
N5–Fe2–N2	88.8(2)	N8–Fe4–N4	89.8(2)
O13–Fe2–N2	81.26(19)	O17–Fe4–N4	80.28(19)
O12–Fe2–N2	153.71(19)	O6–Fe4–N4	109.9(2)
O8–Fe2–N2	109.68(19)	O16–Fe4–N4	150.45(18)

Table S9. Hydrogen bonds for **4** (Å and °)

D–H···A	d(D–H)	d(H···A)	d(D···A)	\angle (DHA)
O1–H1···O25	0.90	2.03	2.800(7)	142.4
O2–H2···O26	0.88	1.97	2.827(6)	164.0
O25–H25···O19	0.82	2.12	2.820(7)	143.0
O26–H26···O22	0.82	2.37	2.833(7)	116.5
O27–H27···O21	0.85	2.13	2.983(9)	179.5

Magnetochemical Analysis Details

In order to model the magnetic characteristics of polynuclear coordination complexes, CONDON implements both (a) isotropic model Hamiltonians for pure spin systems and (b) full model Hamiltonians that act upon the full d or f manifolds and take into account all magnetically relevant single-ion aspects, augmented by exchange terms to model intra- and intermolecular coupling interactions. Note that the use of these models is mutually exclusive, i.e. systems such as the {Fe₄Dy₂} cluster in **1** cannot be calculated as a mixture of spin-only Fe(III) and anisotropic Dy(III) ions.

The isotropic model Hamiltonian (a), used here for compounds **2** and **3**, accounts for Heisenberg-Dirac-van Vleck-type exchange interactions and the Zeeman effect for N spin centers:

$$\hat{H} = \sum_{i < j}^N -2J_{ij} \hat{\mathcal{S}}_i \cdot \hat{\mathcal{S}}_j + g_{eff}\mu_B \sum_{i=1}^N \mathbf{B} \cdot \hat{\mathcal{S}}_i$$

The full model Hamiltonian (b) accounts for the single-ion effects of the individual magnetic centers (with N valence electrons) via

$$\begin{aligned} \hat{H} = & \sum_{i=1}^N \left[-\frac{\hbar^2}{2m_e} \nabla_i^2 + V(r_i) \right] + \sum_{i>j}^N \frac{e^2}{r_{ij}} + \sum_{i=1}^N \xi(r_i) \kappa \hat{l}_i \cdot \hat{s}_i \\ & \hat{H}_0' + \hat{H}_{ee}' + \hat{H}_{SO}' \\ & + \sum_{i=1}^N \sum_{k=0}^{\infty} \left\{ B_0^k C_0^k(i) + \sum_{q=1}^k \left[B_q^k (C_{-q}^k(i) + (-1)^q C_q^k(i)) + i B_q^{ik} (C_{-q}^k(i) - (-1)^q C_q^k(i)) \right] \right\} \\ & + \hat{H}_{LF}' \\ & + \sum_{i=1}^N \mu_B (\kappa \hat{l}_i + 2\hat{s}_i) \cdot \mathbf{B} \\ & + \hat{H}_{mag}' \end{aligned}$$

where \hat{H}_0' represents the energy in central field approximation, \hat{H}_{ee}' the interelectronic repulsion, \hat{H}_{SO}' the spin-orbit coupling, \hat{H}_{LF}' the electrostatic effects of the ligands in the framework of ligand field theory (Wybourne notation), and \hat{H}_{mag}' the Zeeman effect of an external magnetic field. For a complete description of all parameters (see M. Speldrich, H. Schilder, H. Lueken, P. Kögerler, *Isr. J. Chem.*, 2011, **51**, 215). This Hamiltonian is then extended to include suitable coupling expressions; here the exchange interactions between N spin centers are again described by a HDvV-type Hamiltonian:

$$\hat{H} = \sum_{i < j}^N -2J_{ij} \hat{\mathcal{S}}_i \cdot \hat{\mathcal{S}}_j$$

Note that the full model Hamiltonian first acts on the single electron states, while the exchange Hamiltonian acts on the resulting total spin states of each center (the full Russell-Saunders ground term, i.e. 16 states for Dy^{III}, 6 for Fe^{III}) after inclusion of all single-ion effects.

Correlation analysis of exchange energies for compound 3:

In order to establish the (linear) interdependencies of the four exchange energies (J_{1-4}) used to model compound **3** based on an isotropic spin Hamiltonian, the correlation coefficients (Table S10) were calculated. The results show that J_4 (representing the Gd-Gd exchange pathway) has the smallest correlation with the other parameters, and that J_1 and J_3 (representing the Fe-Gd exchange pathways) have the highest correlation.

Table S10. Correlation coefficients ($\rho_{ik} = \text{cov}(J_i, J_k)/[\text{var}(J_i) \cdot \text{var}(J_k)]$) of the fit parameters J_i , to estimate their (linear) interdependencies.

ρ	J_1	J_2	J_3	J_4
J_1	1	+0.706	-0.982	-0.253
J_2	—	1	-0.805	-0.254
J_3	—	—	1	-0.256
J_4	—	—	—	1

Table S11. Magnetochemical analysis details (all energy values in cm⁻¹)

Compound	2, {Fe ₄ Y ₂ }		4, {Fe ₄ Eu ₂ }		3, {Fe ₄ Gd ₂ }		1, {Fe ₄ Dy ₂ }
model type	<i>effective</i>	<i>full</i>	<i>full^b</i>	<i>full</i>	<i>effective</i>	<i>full</i>	<i>full</i>
spin center	<i>S</i> = 5/2	Fe ³⁺ ^a	Fe ³⁺	Eu ³⁺	<i>S</i> = 7/2	Gd ³⁺	Dy ³⁺
<i>F</i> ² (<i>B</i>)	—	825	see 2	90225	—	91800	94500
<i>F</i> ⁴ (<i>C</i>)	—	3300	see 2	63319	—	64425	66320
<i>F</i> ⁶	—	—	—	48413	—	49258	50706
ζ	—	400	see 2	1320	—	1470	1932
<i>B Error!</i>	—	−3.5×10 ³	—	−1.5×10 ²	—	−2.0×10 ²	−3.0×10 ²
<i>B Error!</i>	—	2.40×10 ⁴	—	−1.94×10 ³	—	1.90×10 ³	−1.85×10 ³
<i>B Error!</i>	—	1.90×10 ⁴	—	—	—	—	—
<i>B Error!</i>	—	—	—	2.08×10 ²	—	2.05×10 ²	2.10×10 ²
<i>J</i> ₁	—	—	—	—	−0.38	−0.42	−0.48
<i>J</i> ₂	−6.5	−6.5	−6.3	−6.7	−6.5	−6.5	−6.7
<i>J</i> ₃	—	—	—	—	+0.20	—	—
<i>J</i> ₄	—	—	—	—	+0.03	—	—
$\lambda_{\text{mf}} / \text{mol cm}^{-3}$	—	—	—	—	—	+0.042	+0.075
$\rho / \%$	0.25	0.2	0.4	0.4	—	—	—
<i>SQ</i> / % ^c	1.8	1.0	3.9	1.0	1.2	1.9	1.6

Values of Slater-Condon parameters *F*², *F*⁴, *F*⁶, Racah parameters *B*, *C* and one-electron spin-orbit coupling constants ζ are taken from J. S. Griffith, *The Theory of Transition-Metal Ions*, Cambridge University Press, Cambridge, 1961 and used as constants in the least-squares fitting procedures.

^a Ligand field B^q_k parameters derived for Fe³⁺ for **2** are used as constants in the simulations for **1**, **3**, and **4**.

^b Alternative model description based on the additive contribution of two Fe···Fe dimers (modeled identical to **2**, using the full model Hamiltonian) and the contribution of the two Eu³⁺ centers that here is assumed to be a constant, temperature-independent paramagnetic value ($\chi_{\text{TIP}}(2\text{Eu}^{3+}) = +1.03 \times 10^{-2} \text{ cm}^3 \text{ mol}^{-1}$).

^c The goodness-of-fit parameter *SQ* is defined as $SQ = \sqrt{\frac{1}{n} \sum_{i=1}^n \frac{(\chi_{\text{exp}}(i) - \chi_{\text{calc}}(i))^2}{\chi_{\text{exp}}^2(i)}}$

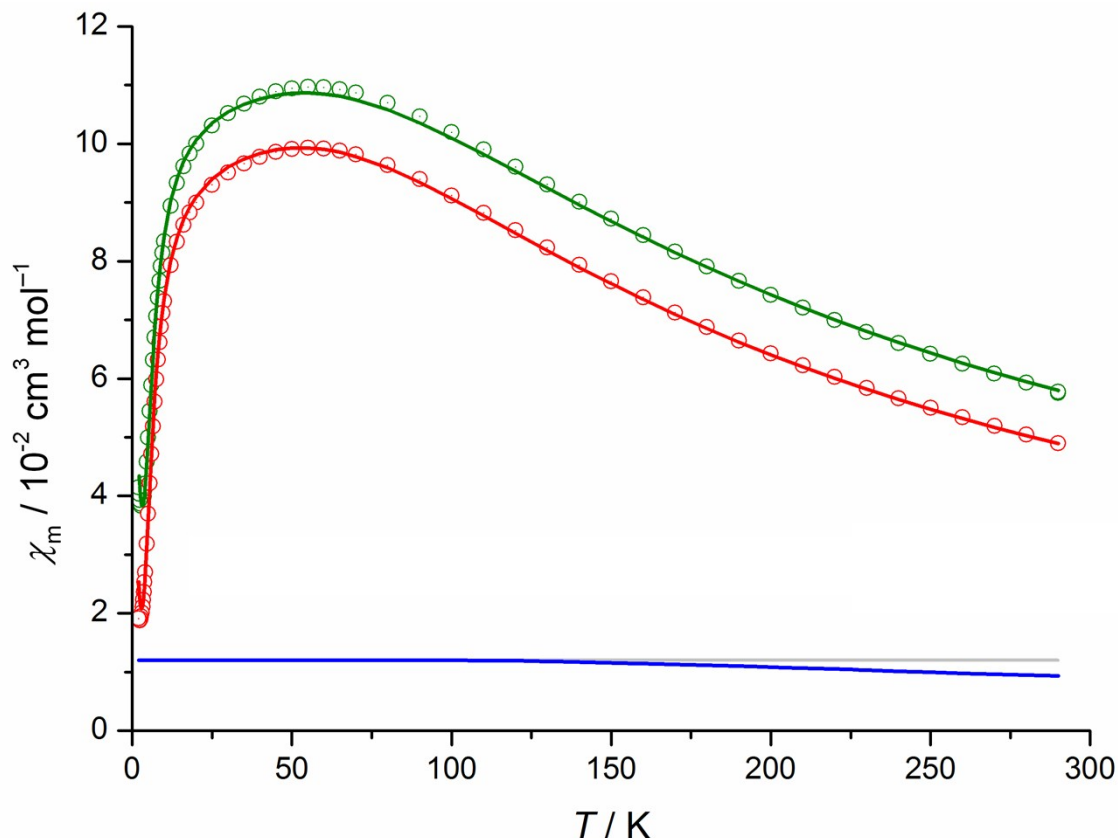


Figure S9. Molar magnetic susceptibility (χ_m) as a function of temperature (0.1 Tesla; open circles, exp. data; solid graphs, least-squares fits) for $\{\text{Fe}_4\text{Y}_2\}$ (2; red) and $\{\text{Fe}_4\text{Eu}_2\}$ (4; green). Blue line: the nearly temperature-independent paramagnetic Eu^{III} single-ion contribution (horizontal gray line: low-temperature TIP value of two Eu^{III} centers).

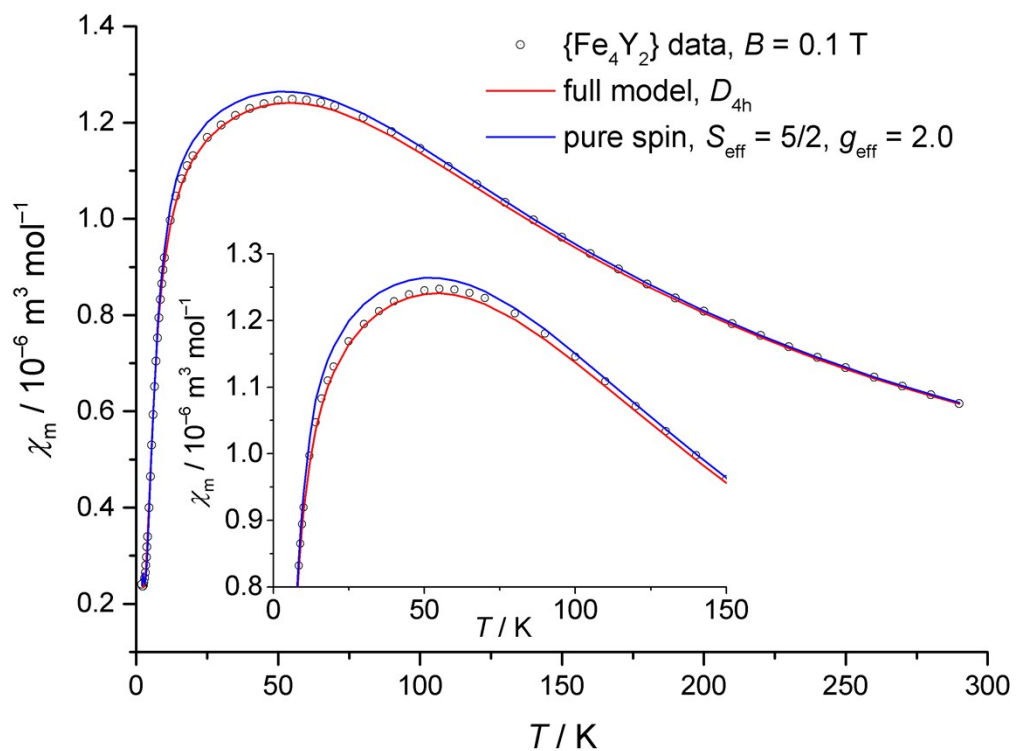


Figure S10. Comparison of least-squares fits for the effective spin-only model (blue graph, SQ = 1.8%) and the full model (red graph, SQ = 1.0%) for the $\{\text{Fe}_4\text{Y}_2\}$ compound **2**. Open circles: experimental data.

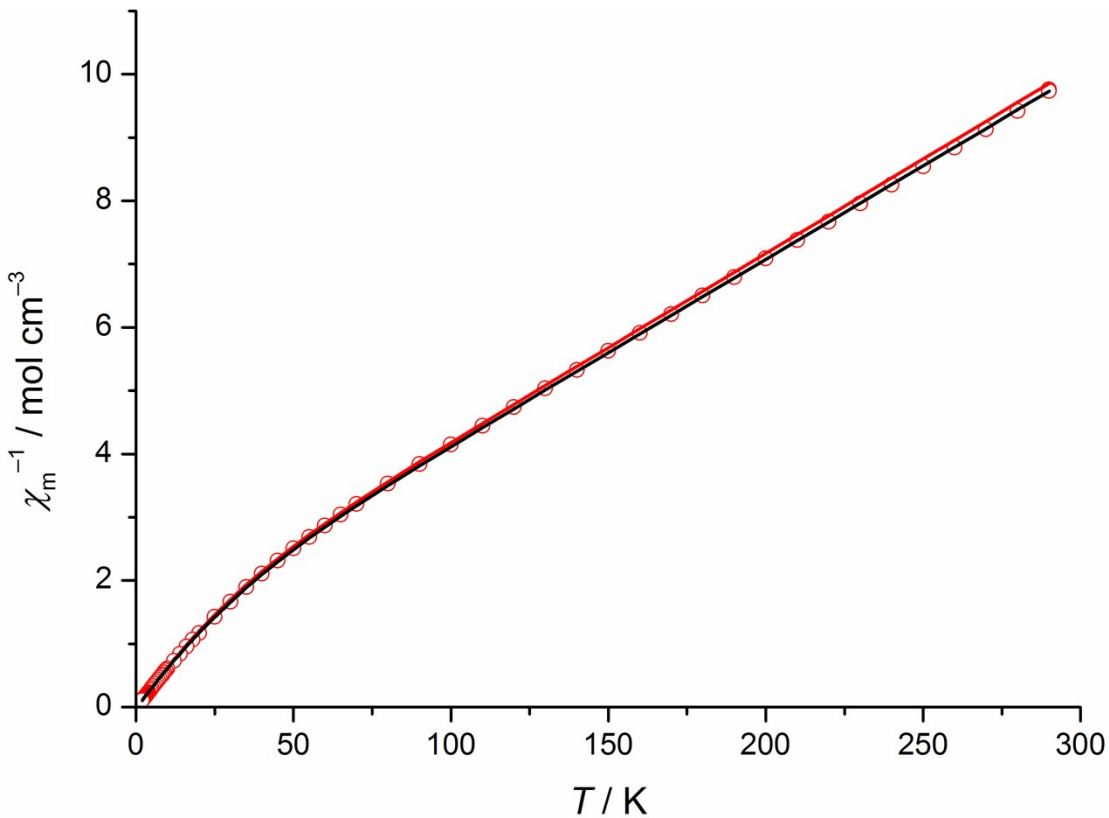


Figure S11. Reciprocal molar magnetic susceptibility as a function of temperature for compound **2**, $\{\text{Fe}_4\text{Gd}_2\}$ at 0.1 Tesla (open circles, exp. data; solid graphs, simulations). Black: effective (pure-spin) $4J$ model; red: dimer of triangles (see Table S10 for parameters). Note that the differences between the two models mostly affect the high-temperature range.

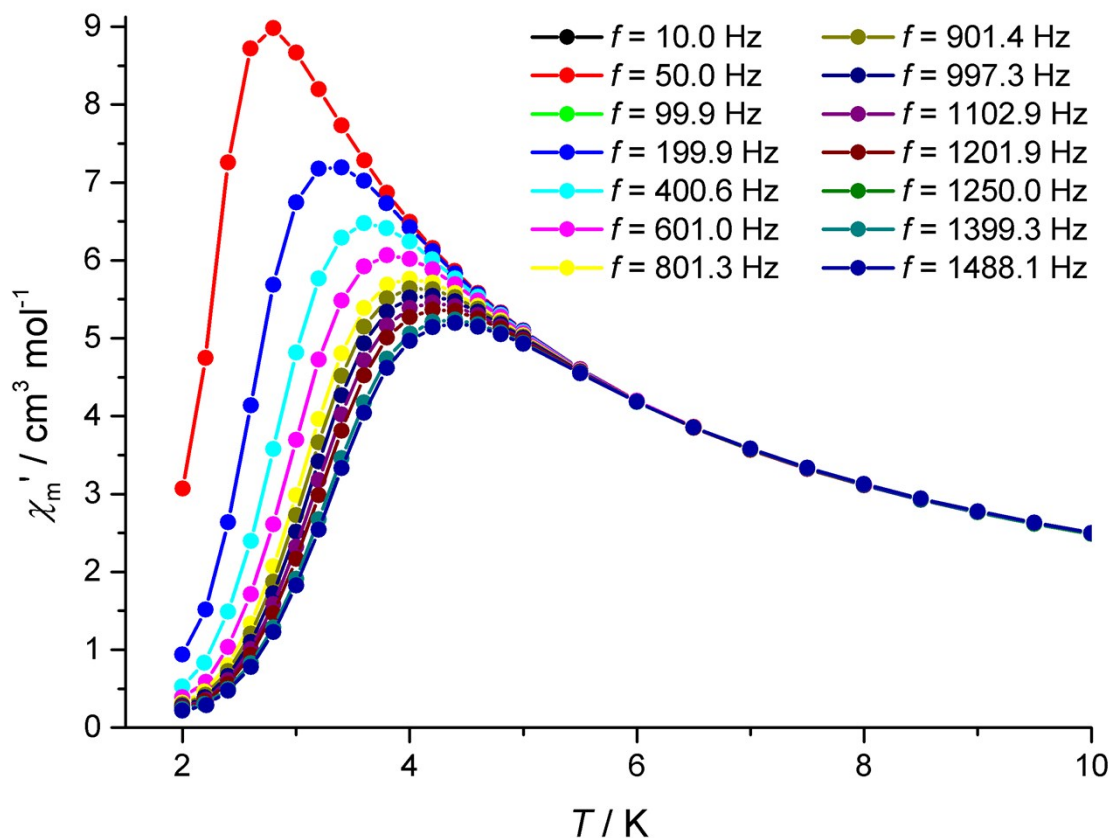


Figure S12. In-phase component χ_m' of the ac magnetic susceptibility data as a function of temperature T at different exciting frequencies f for compound **1**.

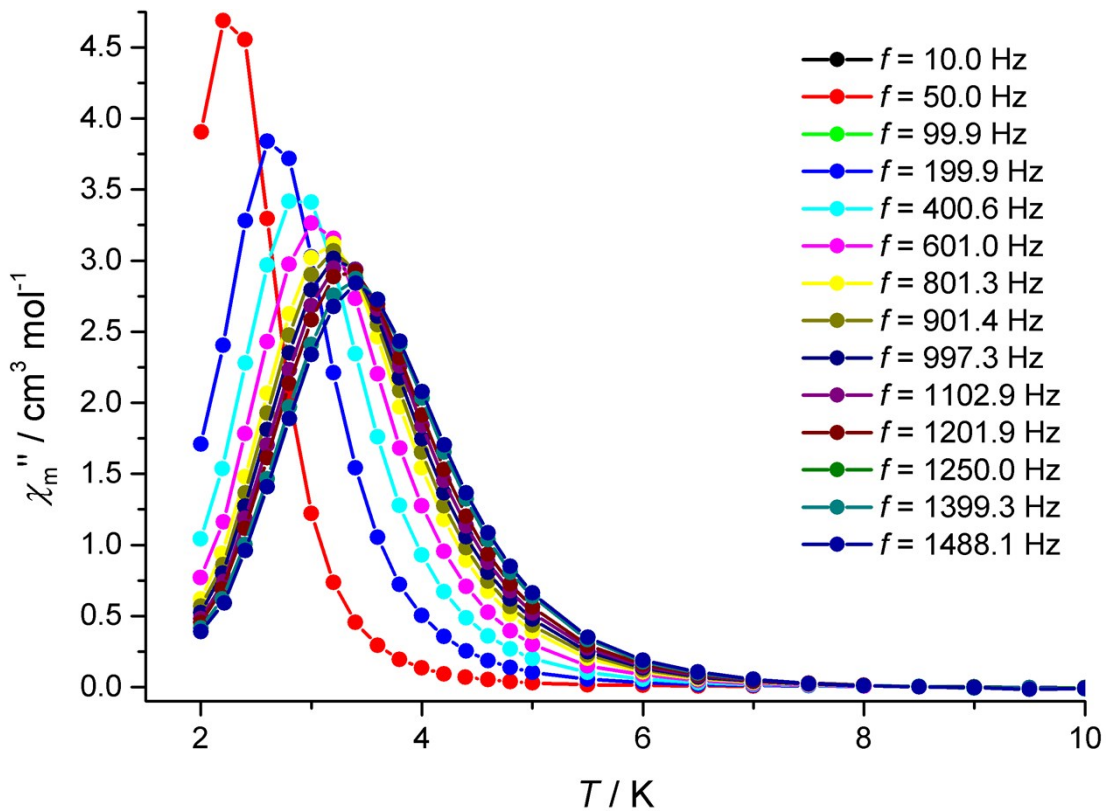


Figure S13. Out-of-phase component χ_m'' of the ac magnetic susceptibility data as a function of temperature T at different exciting frequencies f for compound **1**.

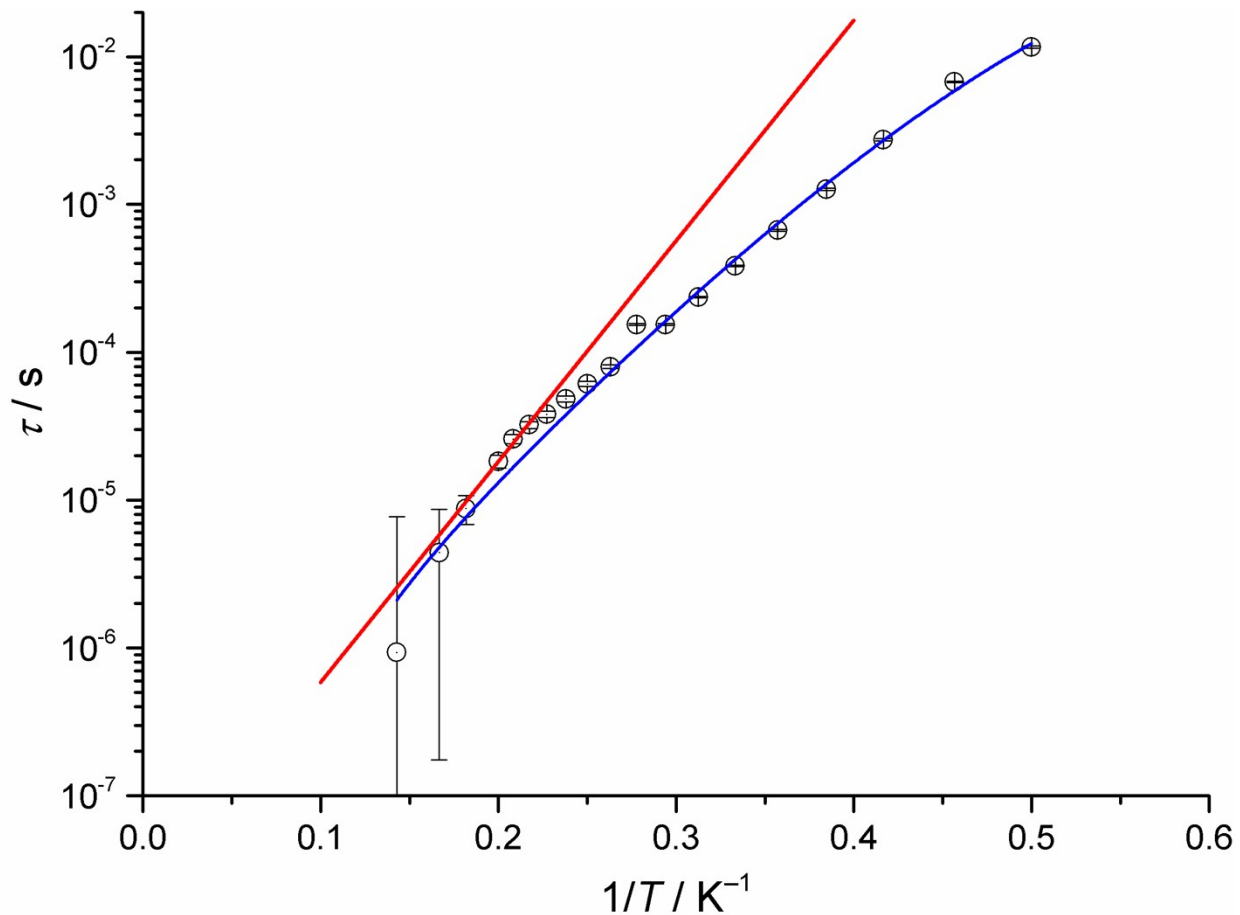


Figure S14. Arrhenius plot to determine the relaxation parameters for two relaxation scenarios: (1) assuming Orbach-type relaxation (red line), yielding an attempt time $\tau_0 = (1.88 \pm 1.14) \times 10^{-8} \text{ s}$ and an effective relaxation barrier energy $\Delta E = (23.9 \pm 2.0) \text{ cm}^{-1}$; (2) assuming both Orbach and Raman relaxation processes, resulting in $\tau_0 = (1.01 \pm 0.89) \times 10^{-7} \text{ s}$, $\Delta E = (18.4 \pm 2.7) \text{ cm}^{-1}$, $n = 6.6 \pm 0.4$, $C = (0.66 \pm 0.23) \text{ K}^{-n} \text{ s}^{-1}$.

Table S12. Fit parameters to generalized Debye expression for compound **1**. Note that the distribution width of τ is quantified by the scalar parameter α in the generalized Debye model where a deviation from $\alpha = 0$ indicates multiple relaxation times due to multiple relaxation mechanisms. Averaged over all isotherms, the mean value of α here results as 0.131 (± 0.070).

T / K	$\chi_s / \text{cm}^3 \text{ mol}^{-1}$	$\chi_T / \text{cm}^3 \text{ mol}^{-1}$	α	τ / s
2.0	0.058	15.869	0.230	1.162×10^{-2}
2.2	0.020	15.527	0.242	6.736×10^{-3}
2.4	0.042	13.261	0.229	2.745×10^{-3}
2.6	0.121	11.468	0.207	1.267×10^{-3}
2.8	0.207	10.229	0.191	6.677×10^{-4}
3.0	0.311	9.276	0.175	3.840×10^{-4}
3.2	0.389	8.535	0.162	2.365×10^{-4}
3.4	0.448	7.931	0.152	1.541×10^{-4}
3.6	0.448	7.931	0.152	1.541×10^{-4}
3.8	0.896	6.951	0.116	7.984×10^{-5}
4.0	1.081	6.553	0.102	6.106×10^{-5}
4.2	1.298	6.197	0.086	4.843×10^{-5}
4.4	1.386	5.884	0.078	3.801×10^{-5}
4.6	1.636	5.594	0.059	3.226×10^{-5}
4.8	1.666	5.339	0.051	2.586×10^{-5}
5.0	1.272	5.105	0.053	1.826×10^{-5}
5.5	0.601	4.604	0.043	8.775×10^{-6}
6.0	0.039	4.197	0.039	4.408×10^{-6}
7.0	-2.304	3.571	0.033	9.341×10^{-7}

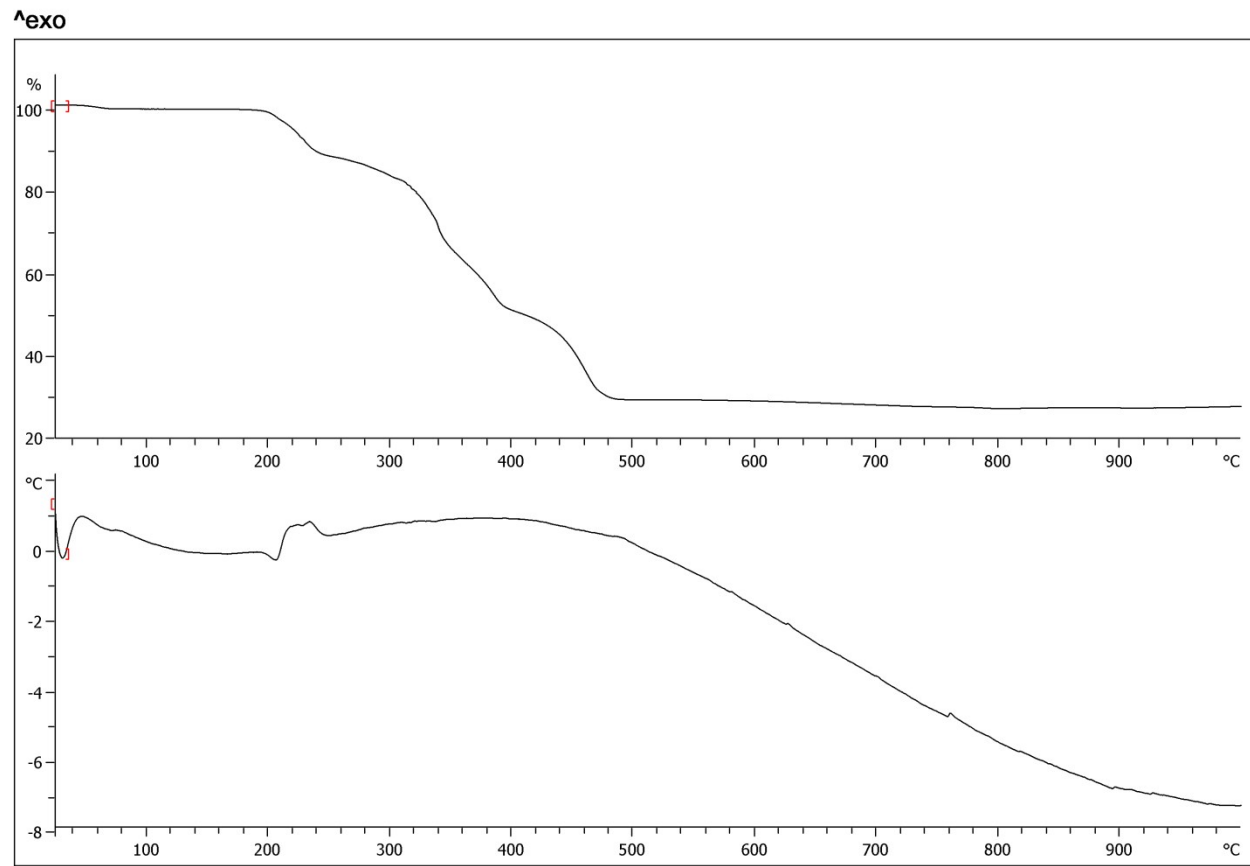


Figure S15. TGA/DTA curve for compound **1**.

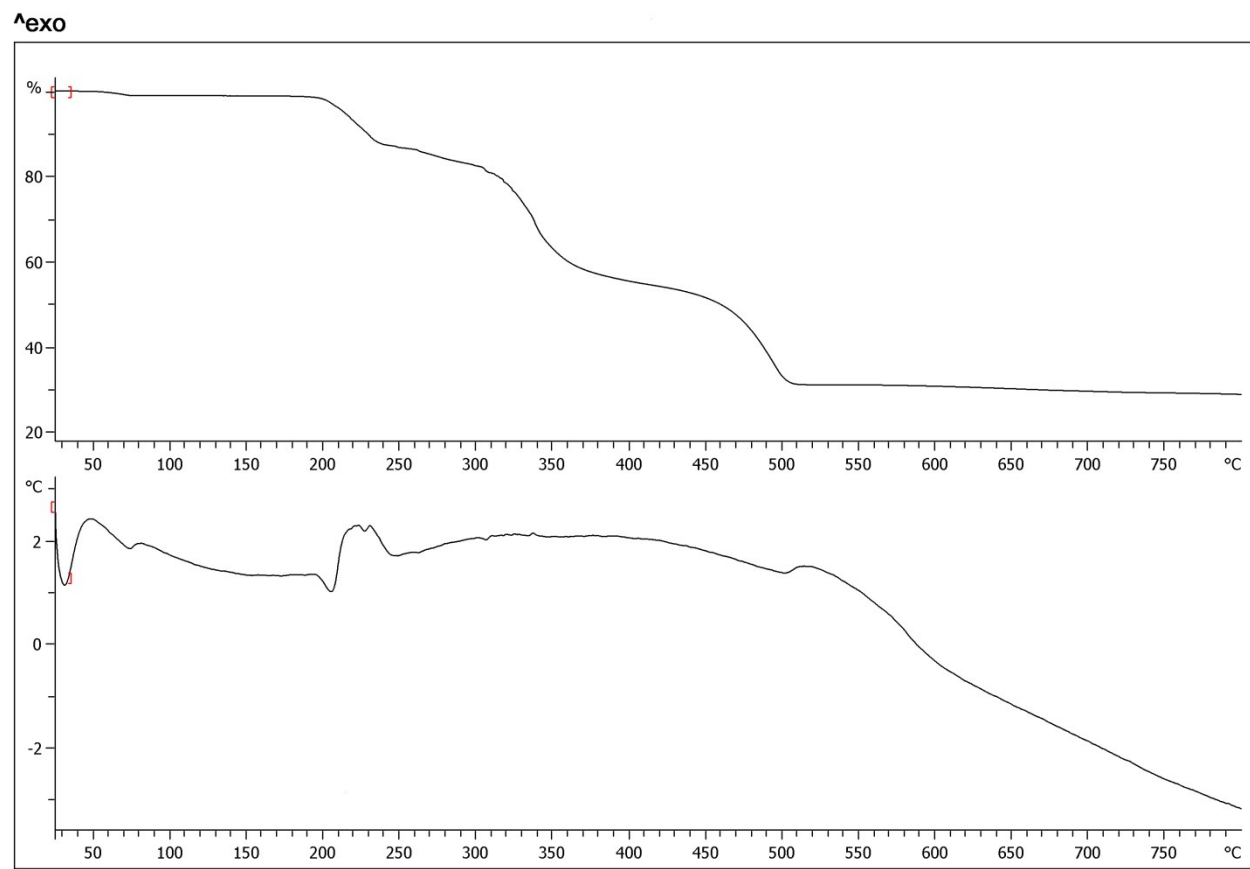


Figure S16. TGA/DTA curves for compound 2.

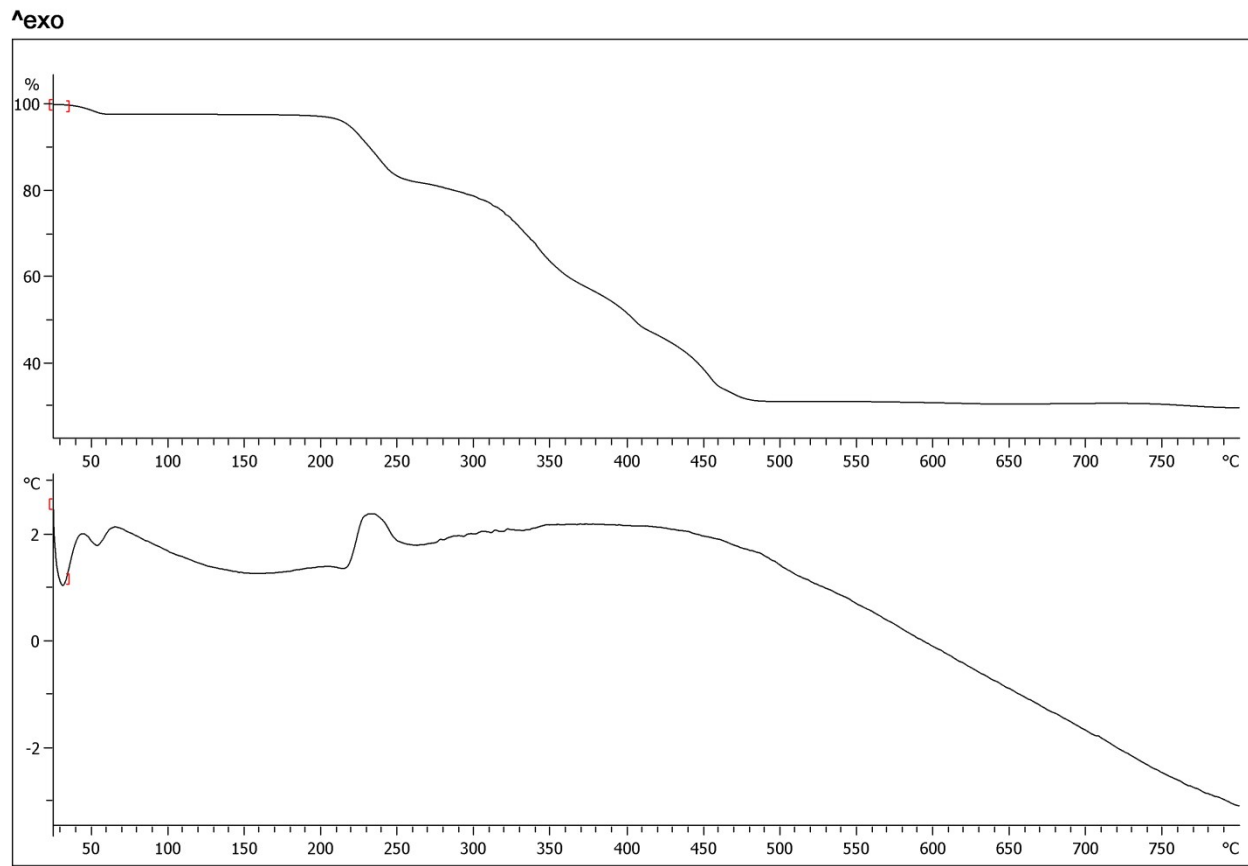


Figure S17. TGA/DTA curves for compound 3.

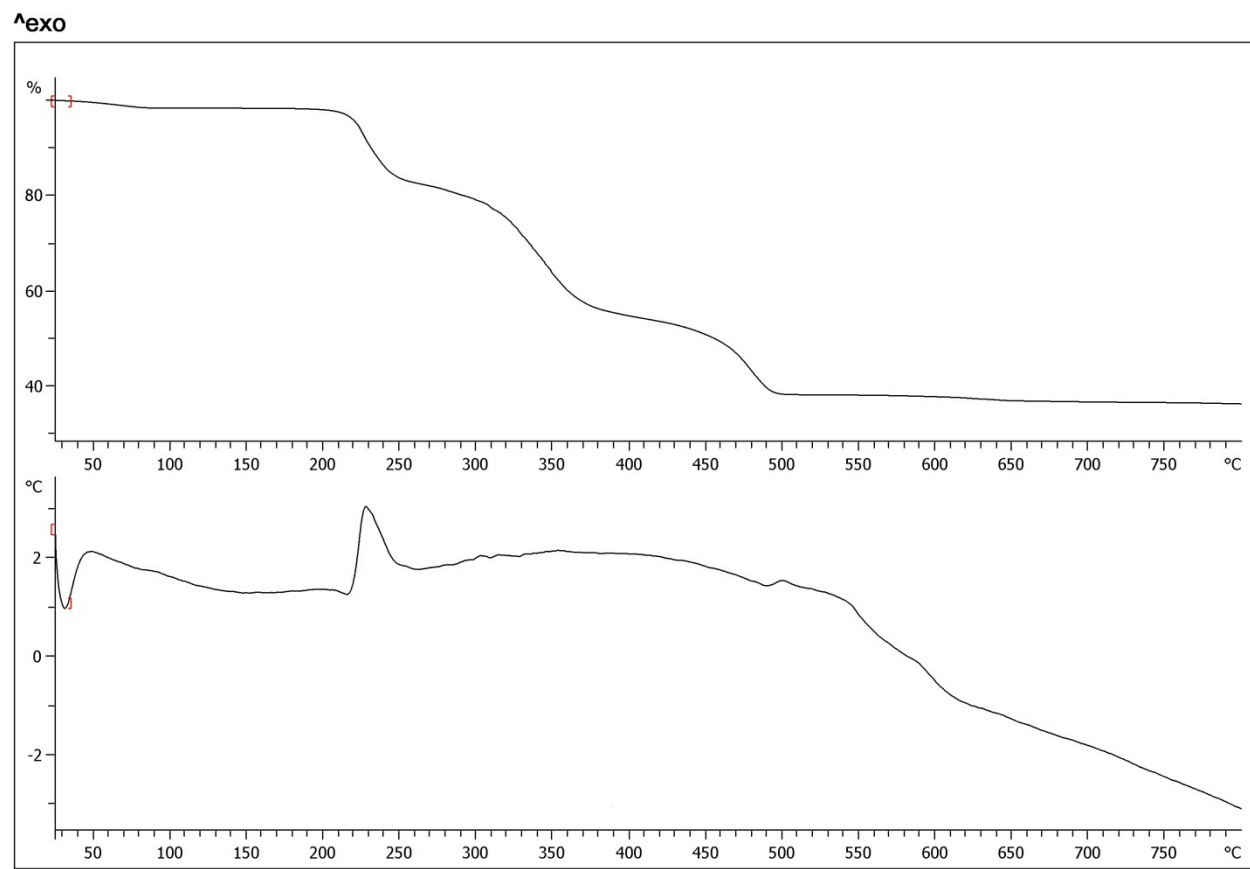


Figure S18. TGA/DTA curves for compound 4.